Heat transfer from spiral tubes in an air fluidized bed
by David Walter Everly

A thesis submitted in partial fulfillment of the requirements for the degree of MASTER OF SCIENCE in Chemical Engineering
Montana State University
© Copyright by David Walter Everly (1978)

Abstract:
The primary objective of this investigation is to present information on heat transfer from spiral copper tubes to an air fluidized bed. A cylindrical Plexiglass column, 14 inches in diameter and 12 feet in height, and glass beads as the solid particles were used. The experimental variables were particle diameter (0.0076 inches to 0.0164 inches), air flow rate (65 pounds per hour to 550 pounds per hour), and number of ridges (3,5) on the spiral copper tubes. A coiled configuration of the spiral tubes was used. The heat transfer coefficients increased with decreasing particle diameter and increasing air flow rate. For the smaller diameter particles, a leveling off or maximum of heat transfer coefficients was observed at higher air flow rates. The spiral tube with three ridges had higher heat transfer coefficients than the one with five ridges. However, the comparative performance to bare tubes was similiar for both spiral tubes. A 45 per cent increase in performance over bare tubes using spiral tubes and the 0.0164 inch diameter particles was recorded. A correlation was formulated which fit the data within the range of experimental error.

STATEMENT OF PERMISSION TO COPY

In presenting this thesis in partial fulfillment of the requirements for an advanced degree at Montana State Univeristy, I agree that the Library shall make it freely available for inspection. I further agree that permission for extensive copying of this thesis for scholarly purposes may be granted by my major professor, or, in his absence, by the Director of Libraries. It is understood that any copying or publication of this thesis for financial gain shall not be allowed without my written permission.

Signature David Walter Everly

Date 2/24/78

HEAT TRANSFER FROM SPIRAL TUBES IN AN AIR FLUIDIZED BED

by

DAVID WALTER EVERLY

A thesis submitted in partial fulfillment
of the requirements for the degree

of

MASTER OF SCIENCE

in

Chemical Engineering

Approved:

William E Lenitz
Chairperson, Graduate Committee

Lloyd Berg
Head, Major Department

Henry L Parsons
Graduate Dean

MONTANA STATE UNIVERSITY
Bozeman, Montana

February, 1978

ACKNOWLEDGMENT

The author acknowledges the staff of the Chemical Engineering Department and the Graduate Committee for their time and effort.

Special acknowledgment is given to William Genetti for his guidance throughout the project.

The funding for this research was provided by the National Science Foundation.

TABLE OF CONTENTS

LIST OF TABLES

LIST OF FIGURES

ABSTRACT

The primary objective of this investigation is to present information on heat transfer from spiral copper tubes to an air fluidized bed. A cylindrical Plexiglass column, 14 inches in diameter and 12 feet in height, and glass beads as the solid particles were used. The experimental variables were particle diameter (0.0076 inches to 0.0164 inches), air flow rate (65 pounds per hour to 550 pounds per hour), and number of ridges (3,5) on the spiral copper tubes. A coiled configuration of the spiral tubes was used. The heat transfer coefficients increased with decreasing particle diameter and increasing air flow rate. For the smaller diameter particles, a leveling off or maximum of heat transfer coefficients was observed at higher air flow rates. The spiral tube with three ridges had higher heat transfer coefficients than the one with five ridges. However, the comparative performance to bare tubes was similiar for both spiral tubes. A 45 per cent increase in performance over bare tubes using spiral tubes and the 0.0164 inch diameter particles was recorded. A correlation was formulated which fit the data within the range of experimental error.

INTRODUCTION

Fluidized beds have an increasing number of applications in a wide range of industrial operations. Several applications are drying, calcining, mixing, cooling towers, catalytic reactors, coating, and removal of fines from bed particles. A fluidized bed is a column that contains solid particles that rest on a distributor plate at the bottom of the column. A fluidizing mass, gas or liquid, is passed up through the bottom of the column. Starting with low mass velocities of a gas, for example, passing up through the bed, there is no movement of the solid particles. As the gas velocity is increased, the pressure drop across the bed increases. At the point when the pressure drop across the bed of solid particles equals the weight of the solid particles and the friction of the particles at the side of the column, the bed will expand. This is called the minimum fluidization velocity. The particles separate and some particle movement begins, but there is no bubbling. After this point, an increase in gas velocity causes the particles to separate more forming larger pores and channels in the bed. Bubbles now begin to rise through the bed. As the bubbles rise, they expand and burst at the surface of the bed. The bed now visually resembles a contained "boiling

liquid"(1). The expansion in the bed is not uniform.

The size and number of bubbles increase as the gas flow increases and also as the height above the distributor plate increases. This is also a function of the geometry of the bed, column diameter, and distributor plate design(2). There is vigorous bubbling in the bed and mixing of the solid particles. This is known as the aggregative or "bubble" regime, the type of fluidization encountered in most applications. As fluidizing mass velocities are increased still further, the bed becomes unstable resulting in massive slugging and surges. This can increase to the point where the solid particles are blown out of the top of the column.

The chemical and petroleum industries use fluidized beds as a catalytic reformer(3), catalytic cracking. Gasification of powdered coal for combustion and conversion has fluidized bed application. Fluidized beds are being used in coating of metal parts with thermoplastic resins, a heat exchanger for geothermal energy, water purification, waste heat and nuclear waste disposal, and the drying of iron ore.

Some of the physical advantages of a fluidized bed are uniform temperature and solid particle mixing

throughout the bed (much higher heat transfer coefficients than forced convection), drying of solid particles, gas mixing, removal of fines from bed particles, and ability to continually recycle or add solid particles to the bed. Another advantage is low capital and maintainence costs. Since a fluidized bed is a stable system that can be operated at steady state, ease of operational control is important. Flexibility of materials that may be used is another advantage.

There are also some disadvantages that are characteristics of fluidized beds. The very active particle movement may cause erosion of column walls, immersed surfaces, and the solid particles. Difficulty is found in fluidization of very sticky materials that can be used in a fluidized bed operating in the bubble regime.

There are many applications where heat is extracted or added to the fluidized bed. This was originally accomplished by heat transfer through the walls of the column. Later, tubes were immersed in the fluidized bed for heat transfer because of the increased surface area. Much research has been done in this area in an effort to establish reliable design criteria. Some research has

been done using tubes with extended surfaces. It has been possible to improve heat transfer rates with extended surfaces. The purpose of this investigation is to present information on the heat transfer coefficients of spiral copper tubing. The spiral copper tubing has previously been used in heat exchanger applications.

THEORY AND PREVIOUS RELATED RESEARCH

The section on theory and previous related research has been divided into the mechanism of fluidization for heat transfer and previous related research.

Mechanism of Fluidization for Heat Transfer

The study of the aggregative or "bubble regime in fluidized beds, including bubble size and behavior and solid particle motion, has been done by several reseachers (3,4,5,6). These include attempts to model analytically the physical characteristics of a fluidized bed. The models have different ranges where the nonideal behavior of a fluidized bed is considered. Mass transfer and heat transfer in fluidized beds cannot necessarily be described by the same model. There have been several models proposed for heat transfer between fluidized beds and surfaces.

A "film" model presented by Levenspiel and Walton(4) describes a thin laminar film of fluidizing gas next to the surface which is the controlling heat transfer resistance. The activity of the solid particle against this film is the model's explanation of increased heat transfer coefficients. A "packet" model presented by Mickley and Fairbanks(8) is described as "packets" of particles coming into contact with the surface for a short

time period, unsteady state heat transfer is the controlling resistance. The "packet" then leaves the surface and returns to the bulk medium to dissipate the heat.

A modification of this theory was presented by Ziegler, Koppel, and Brazelton(9) and extended by Genetti and Knudsen (10). Assuming constant physical properties of the solids and fluids and spheres of uniform diameter for the solid particles, the mechanism proposes that particles from the bulk medium at temperature T_b come into contact with the surface at temperature T_w. Heat is transfered by convection from the surrounding fluid to the particle for a length of time, θ. The fluid temperature, T_f, is assumed to be the arithmetic mean of T_w and T_b. After time θ, the particle returns to the bulk medium to dissipate the heat. This mechanism is shown on Figure 1. The conduction heat transfer at the point of contact with the surface and the radiant heat transfer from the surface are neglected. They found that the following formula describes the rate of heat transfer from a surface in a fluidized bed.

$$Nu_p = \frac{h_o D_p}{k_g} = \frac{7.2}{\left[1 + \frac{6 k_g \theta}{\rho_s C_{ps} D_p^2}\right]^2}$$

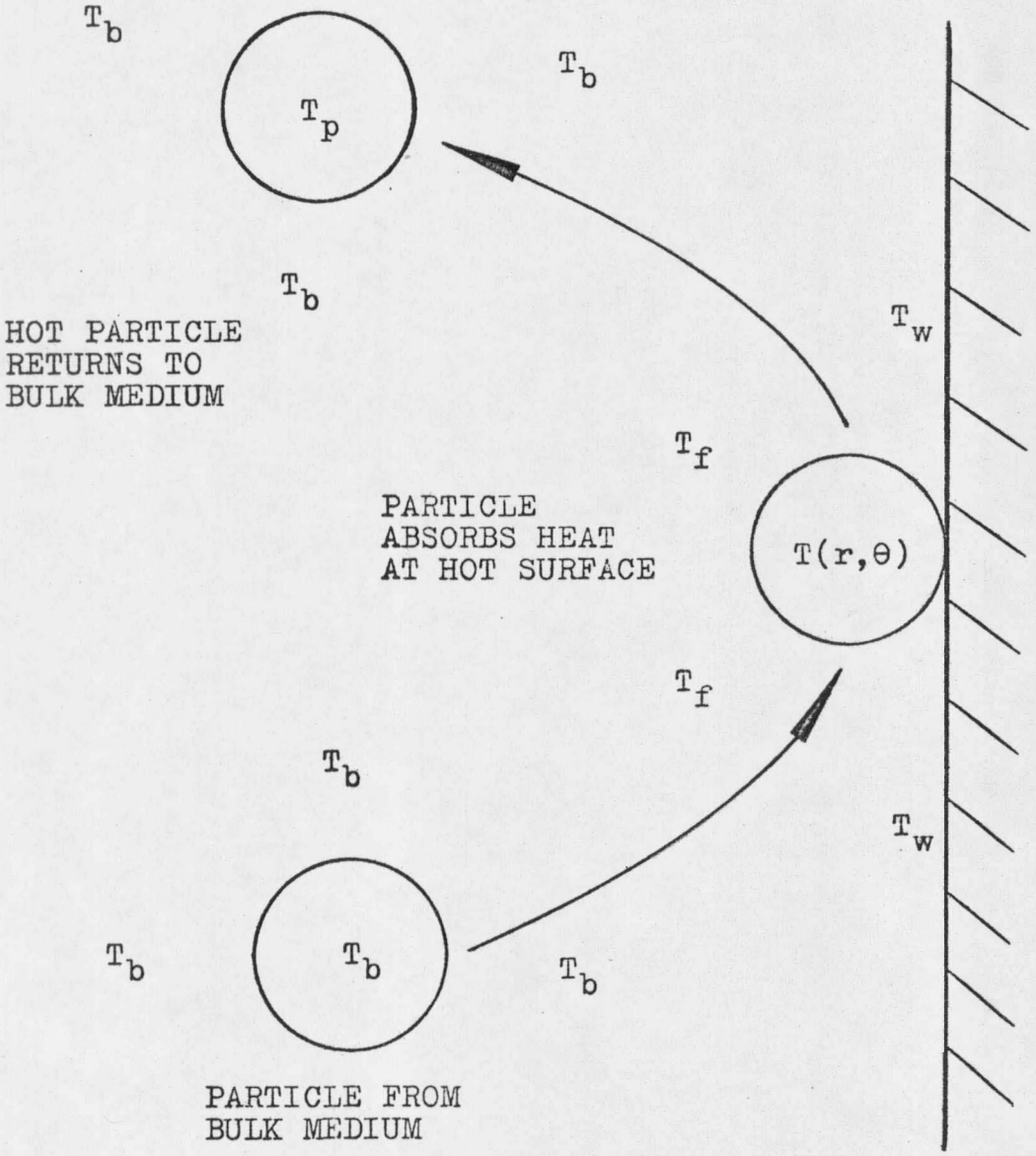

FIGURE 1. PROPOSED HEAT TRANSFER MECHANISM

where,

Nu_p = particle Nusselt number, dimensionless

h_o = heat transfer coefficient, BTU/ft^2-hr-^oF

D_p = particle diameter, ft

k_g = thermal conductivity of fluidizing medium, BTU/hr-ft-^oF

θ = average contact time, hr

ρ_s = density of solid particles, lbs/ft^3

C_{ps} = heat capacity of solid particles, BTU/lb-^oF

Genetti and Knudsen recommended that $10(1-\epsilon)^{0.5}$ be substituted for 7.2 in the above equation, where $(1-\epsilon)$ is the particle fraction, dimensionless. The data collected in this study was correlated using this formula. Kunii and Levenspiel(3) have compared models and suggested a general model which includes the different mechanisms.

Previous Related Research

There have been numerous papers published that have information concerning heat transfer from immersed surfaces. Most papers include a study of the effect of particle diameter. Other work includes studies of the effect of particle shape, density, and heat capacity, fluid thermal conductivity, viscosity, void fraction, and mass velocity. Chen and Withers(13,14) studied the heat transfer character-

istics of vertical bare and finned tubes in a fluidized bed varying fin height and fin spacings. They report that gains as large as 190 per cent for heat transfer coefficients for helical copper fin tubes compared to plain tubes.

Bartel and Genetti(15) studied heat transfer from a horizontal bundle of carbon steel bare tubes and finned tubes to a bed of glass beads fluidized with air. Varying parameters were fin height, distance between tubes, particle diameter, and air mass velocity. Gains up to 80 per cent compared to bare tubes were observed. Priebe and Genetti (16) studied heat transfer from horizontal discontinuous finned tubes and spined tubes as a function of spines per turn and spine height. For copper spines, gains up to 60 per cent were observed.

Kratovil(17) studied heat transfer from a horizontal bundle of continuous, helical copper finned tubes as a function of fin height, fin spacing, and particle diameter. Gains as large as 190 per cent compared to bare tubes were recorded for certain conditions.

EXPERIMENTAL PROGRAM

The primary objective of this investigation was to determine the effect of the number of ridges and the magnitude of the heat transfer coefficients of the spiral copper tubes. The parameters that should effect the heat transfer coefficients are the properties of the fluidized bed, the operating conditions, and the geometry of the equipment. The properties of the fluidized bed are the solid particle size, shape, and composition and the fluidizing medium. The operating conditions are the velocity of the fluidizing medium, the height of particles in the bed, and the inlet temperature and mass flow rate of the medium used to transfer heat from inside the spiral copper tubes. The equipment geometry includes the diameter, the number and depth of the ridges, and the location of the spiral copper tubes and the shape of the column. Four of these parameters are the experimental variables: particle size, velocity of the fluidizing medium, the number of ridges on the spiral copper tube, and the mass flow rate of the medium used to transfer heat from inside the copper tubes.

Air was used as the fluidizing medium. The inlet air temperature was consistantly in the range of 98 ^{o}F to 115 ^{o}F, therefore, the physical properties of the inlet air to the column were nearly constant. Spherical glass beads were

used as the bed particles. The density of the glass is approximately 155 lbs/ft^3, and the glass beads were screened before the final data was collected. Water was used as the medium transferring heat from inside the spiral copper tubes. Data was collected for two different spiral copper tubes (3,5 ridges). The following table is a list of the physical characteristics of the spiral tubes used in this study.

Table 1. Description of Spiral Tubes

	Tube 1 (HTRI 1)	Tube 2 (HTRI 16)
wall thickness	20 gauge	20 gauge
material	copper	copper
length	6 ft (including short plain ends)	6 ft (including short plain ends)
number of ridges	5	3
pitch	2 inches	2.8 inches
groove depth	.15 inches	.21 inches
outer diameter	1-1/8 inch OD	1-1/8 inch OD

The number of ridges on the spiral tubes includes a variable distance between the ridges. This distance was not given in the manufacturer's description of the tubes, but there was sufficient data for each tube to calculate a value for this distance. The distance between ridges was

was calculated as .3513 inches for Tube 1 and .7069 inches for Tube 2. This variable was included in determining the final correlation. The range of the four experimental variables is given in Table 2.

Table 2. Range of Experimental Variables

Variable	Range
Particle size	.0076,.0109,.0164 inch diameter
Air mass velocity	60 to 560 lbs/hr-ft^2
Number of ridges	3,5
Water flow rate	95 to 540 lbs/hr

All of the other parameters were held at constant values which will be described in the following.

EXPERIMENTAL EQUIPMENT

The equipment used in this investigation is divided into three types: the fluidizing system, the thermocouple system, and the tube and water heating system. A schematic drawing of the overall experimental system is shown in Figure 2. A photograph of the column and surrounding equipment is shown on Figure 3.

Fluidizing System

The main parts of the fluidizing system are the column, funnel, distributor plate, air blower, and glass beads.

The column was constructed of a cylindrical, clear Plexiglass that was 3/8 inch thick. The column was 13-1/2 inches inside diameter and 8 feet 9 inches in height. A detail view of the column is shown on Figure 4. The column was divided into two sections that could be separated to make it possible to change the spiral tubes. The lower section was 25-3/4 inches and the upper section was 79-1/4 inches. A 1-3/4 inch flange of 3/4 inch thick Plexiglass was connected to the ends of each section to enable the sections to bolt together. All sections of the column were fitted with rubber gaskets. The top of the column was a removable 1-3/4 inch wooden ring, 3/4 inch thick, with a 13-1/2 inch inside diameter. The center of the lid was covered with

stainless steel screen (1/32 inch openings). To aid in removing the glass beads between runs, a 4-1/2 inch inside diameter port (made of 1/4 inch Plexiglass) was connected to the wall of the column. The column was supported by a wooden frame that was bolted to a concrete floor.

A funnel section made of 1/32 inch galvanized steel was used as the bottom of the column. The cone section of the funnel had a top inside diameter of 13-1/2 inches, a bottom inside diameter of 2 inches, and a height of 10 inches. The spout of the funnel was 2 inch diameter and 4 inches in length.

The distributor plate consisted of a piece of 100 mesh stainless steel wire cloth between two 1/16 inch stainless steel perforated plates (perforations were 1/8 inch diameter and 3/16 inch center-to-center). The distributor plate was 17 inches in diameter and was fitted with rubber gaskets. A particle drain pipe, 1 inch outside diameter, was connected to the distributor plate and extended through the side of the funnel section. A quick opening valve on the end of the pipe was used to empty the column of the glass beads.

Air was supplied to the column with a Sutorbilt blower driven by a 7½ HP Brown-Brockmeyer electrical motor. The

air was blown through a 2-1/2 inch schedule 40 steel pipe that was connected by a rubber hose to the stem of the funnel section under the column. A gate valve in the main line and a gate valve in a 2 inch bypass line which vented air to the atmosphere were used to regulate the air flow rate. The supply valve was left completely open. The air flow rate was controlled by throttling the bypass valve and it was measured using an orifice and water manometer in the supply line. The orifice had a 1-1/2 inch diameter opening and vena contracta pressure taps. The pressure drop across the orifice was measured with a water manometer. A Duragauge pressure gauge located between the orifice and the column was used to measure the pressure of the air entering the column.

The pressure drop across the fluidized bed was measured with a water manometer. The pressure taps were placed 16 -3/4 inches apart, the lower tap was 2 inches above the distributor plate.

Glass beads were used as the solid particles in the bed. A static bed height of 20 inches was a constant for all runs. An analysis of the glass beads is included in the following material.

Thermocouple System

The lead wires from the seven thermocouples were wired into an eleven position switch box mounted on a panel board. The switch box was connected to a Honeywell chart recorder from which temperatures could be read directly in ^{o}F. The thermocouples were iron-constantan (type J, B and S gauge-30). The location of the three bed thermocouples is shown on Figure 3. A single thermocouple was placed on the outer surface of the Plexiglass column, in the air stream entering the column, and in the inlet and outlet water streams. The thermocouple readings were assumed accurate to $\pm$ 0.5 ^{o}F.

Tube and Water Heating System

Two six foot lengths of the spiral copper tube were fitted together and bent into a 7 inch inside diameter coil. A photograph of the coil for Tube 1 is shown in Figure 5. The upper end of the coil was fitted to a 1 inch diameter steel pipe going through a hole in the column wall, 19 inches above the distributor plate. The lower end of the coiled tube was fitted to a 1 inch diameter pipe that went through a hole in the wall of the column, 2-1/2 inches above the distributor plate, and led to a discharge area where the water flow rate could be measured. This

is measured by weighing the amount of water discharged over a set period of time. The average distance between turns of the coil was 2-3/4 inches. The holes where the inlet and outlet water pipes went through the column walls were sealed with Permatex silicone sealant. Water from an overhead tnak was heated by steam in a countercurrent heat exchanger and used as the inlet water to the coiled tube in the bed.

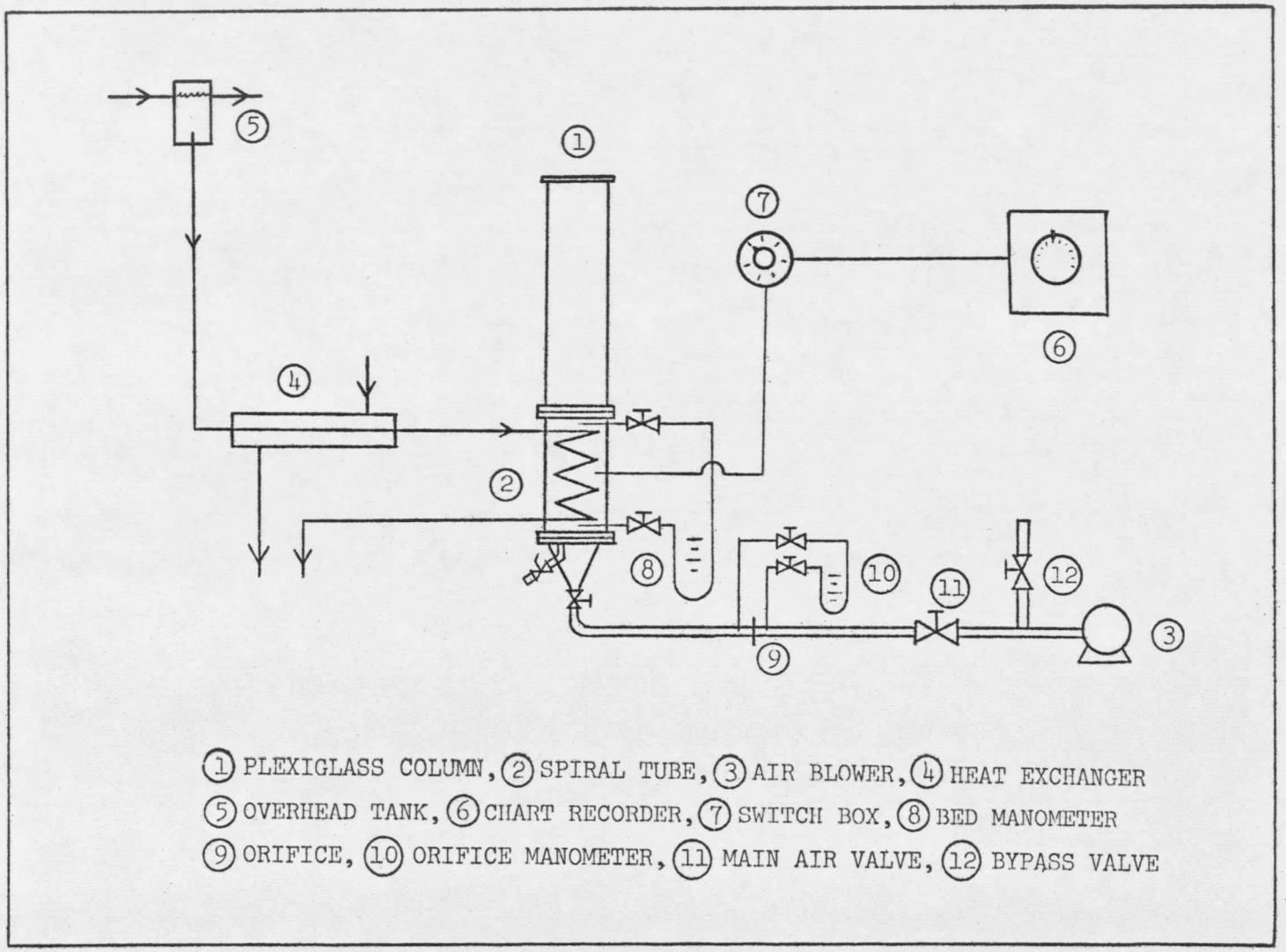

FIGURE 2. SCHEMATIC VIEW OF EQUIPMENT

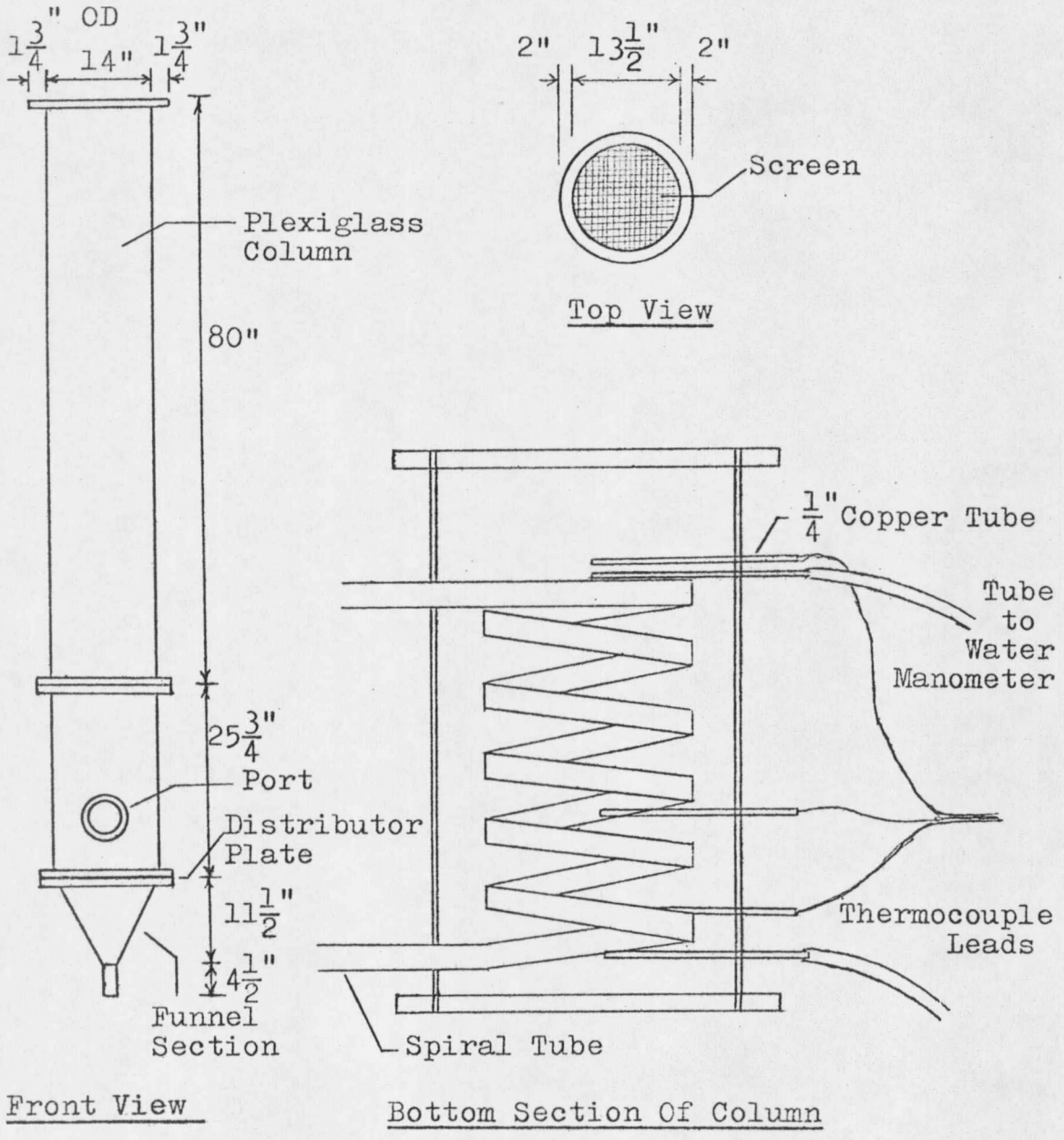

FIGURE 3. DETAIL OF COLUMN

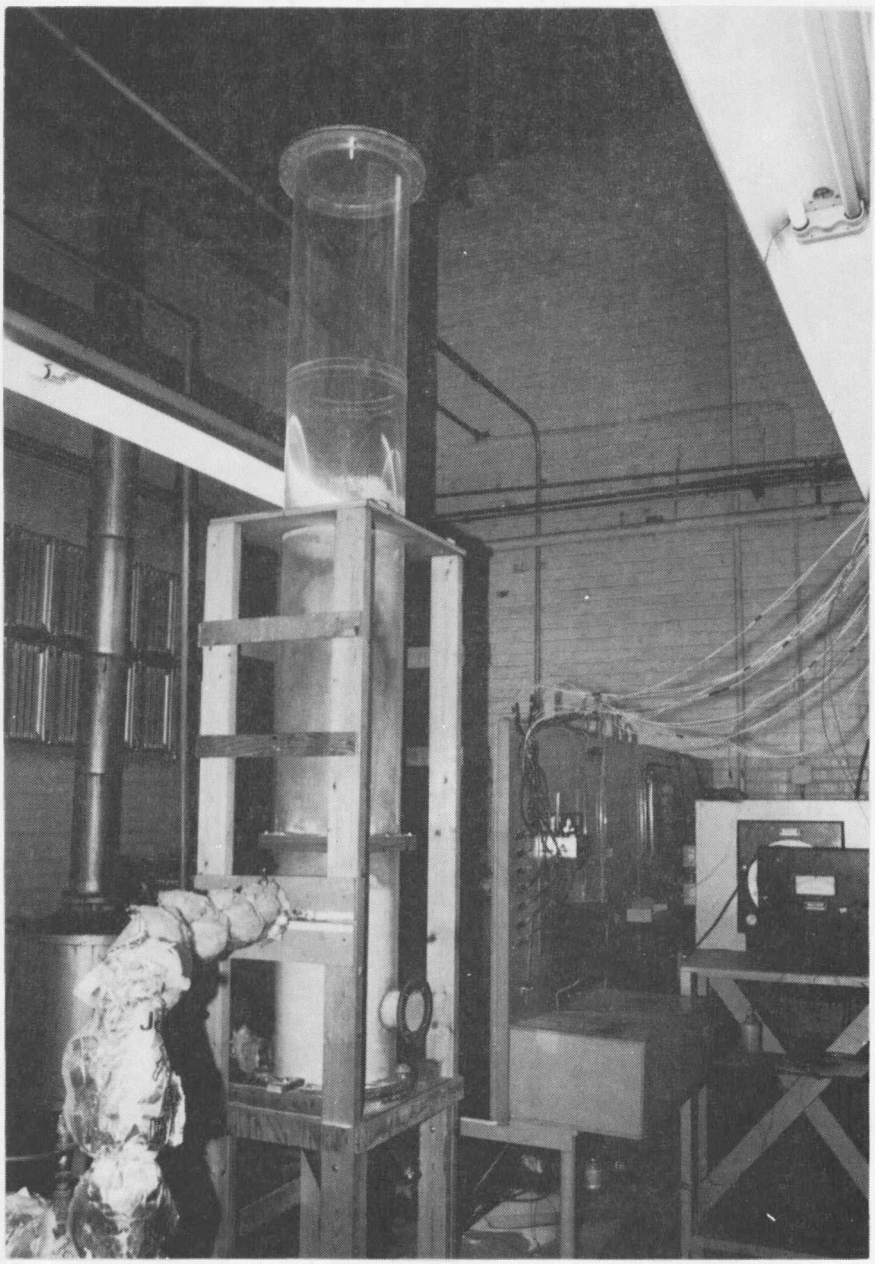

FIGURE 4. COLUMN

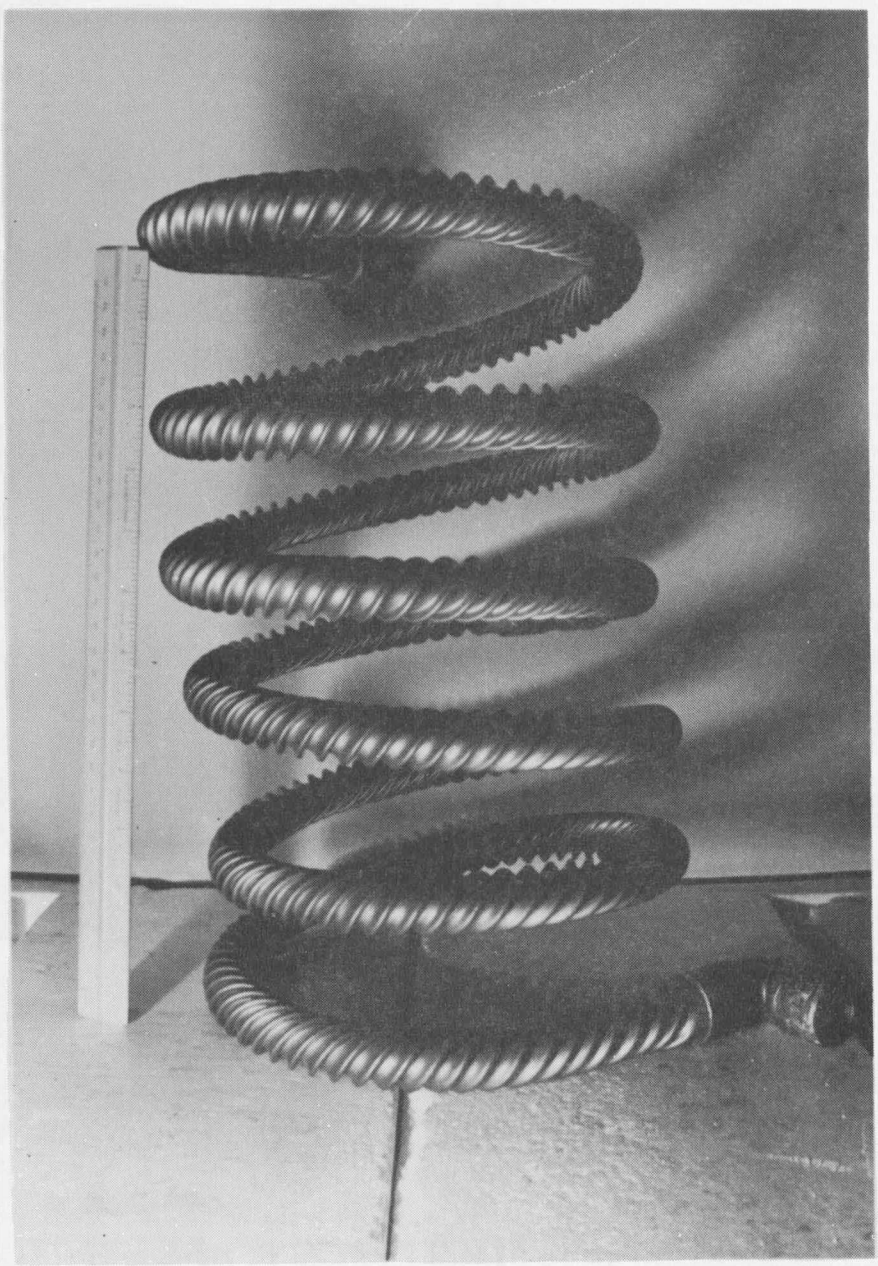

FIGURE 5. SPIRAL TUBE COIL

EXPERIMENTAL PROCEDURE

Minimum Fluidization Velocities

A static bed height of 20 inches above the distributor plate was constant for all runs including determination of the minimum fluidization velocities of the different sized glass beads. The air blower and the heat exchanger were started and the bed was allowed to heat up to the normal operating temperature range. The air flow rate to the column was shut off completely. By throttling the air flow rate until the first sign of bed expansion was visibly detected, the point of minimum fluidization could be found. A micro water manometer was used to measure the air flow rates in this low range. Averages of this method of determinization were used as the experimental minimum fluidizing velocities for the three particle sizes. They were compared with theoretical minimum fluidization velocities predicted by the Leva correlation(5). The experimental minimum fluidization velocities showed deviations of less than 5 per cent from this theoretical correlation. The Leva correlation, which is given in the calculations section, was used in determining G_{mf} for the range of bed temperatures. The calculated G_{mf} was used in the final correlation of data for this investigation.

Glass Bead Analysis

The glass beads were screened in the following ranges: .005-.0098 inch, .0098-.0160 inch, and .0160 inch plus. The density of the glass beads was 155 lbs/ft^3. Using a camera mounted on a microscope, several photographs of random samples of each bead range and a transparent scale were taken. The photograph of the scale was used to determine the average particle diameter of each range of glass beads. The results of this analysis yielded: small particles-.0076 inch diameter, medium particles-.0109 inch diameter, and large particles-.0164 inch diameter. These values agree with the screening ranges for the glass beads. A photograph of a sample of each bead size is given in Figure 6. From these photographs, a spherical particle shape is a reasonable assumption.

Procedure for a Typical Run

The same basic procedure was used for all runs. The spiral copper tube was properly installed in the column and the column was filled to a static height of 20 inches with glass beads of a given diameter. The air blower was started and adjusted to the desired air flow rate. The water flow rate was adjusted to a given operating range.

Varying the steam pressure to the heat exchanger, it was possible to obtain a desired inlet water temperature. This was the most difficult part of each run. Fluctuations in the steam pressure caused fluctuations in the inlet water temperature, which made collecting steady state data very difficult. After the air flow rate was set, the column was allowed to reach steady state, 2-1/2 to 3 hours for the first run and 1-1/2 hours for the following runs at different air flow rates. After reaching steady state, the thermocouple, manometer, and water flow rate data was collected. Three sets of data, spaced by ten minutes, were collected for each run. The average values of this data reduced the error of the inlet water temperature fluctuations.

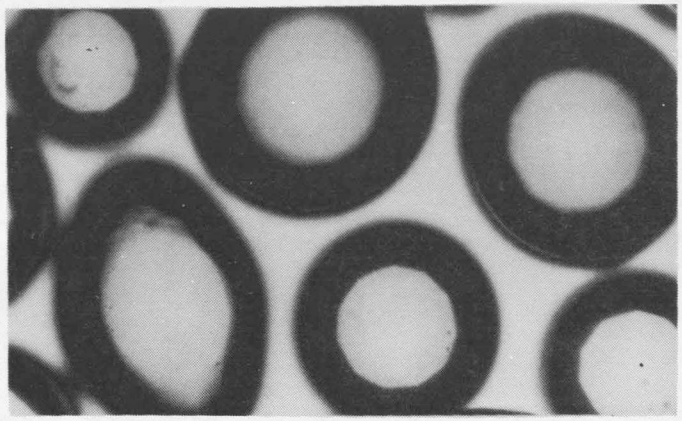

Large- .0164 inches

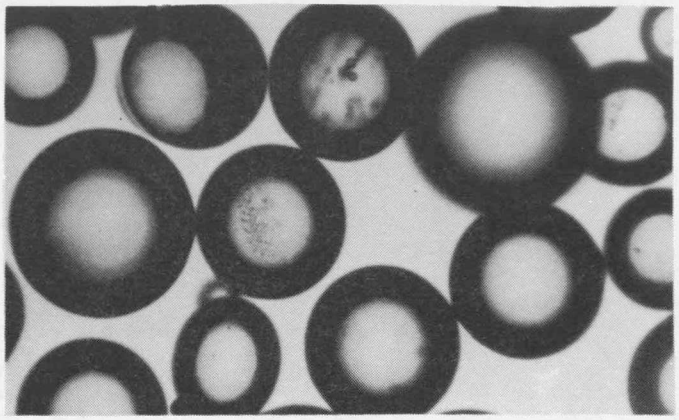

Medium- .0109 inches

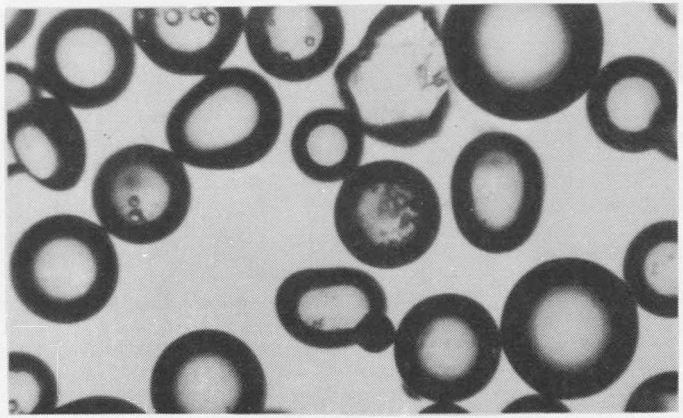

Small- .0076 inches

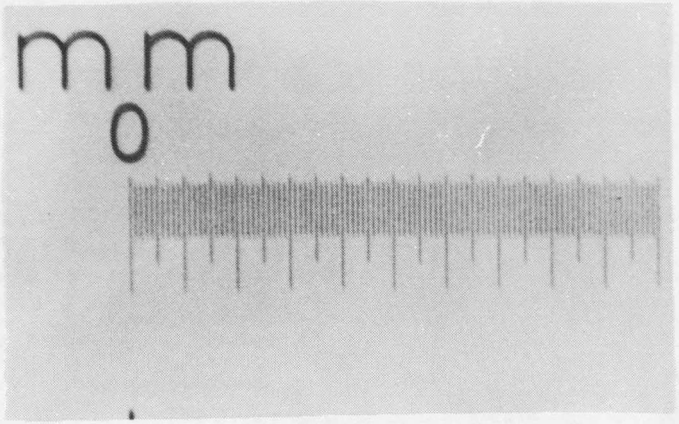

Scale

FIGURE 6. MICROPHOTOGRAPH OF PARTICLES

RESULTS AND DISCUSSION

The primary objective of this investigation is to experimentally study and analyze heat transfer from spiral copper tubes in a fluidized bed. The spiral copper tubes have an increased surface area. The parameters that were varied in this study were air mass velocity, water flow rate, particle diameter, and the number of ridges on the spiral copper tubes. The range of the mass flow rate of air through the bed is 65-550 pounds per hour per square foot. The range of mass flow rate of the water through the spiral tube is 275-375 pounds per hour. There are three different glass bead sizes that were used: small-.0076 inch diameter, medium-.0109 inch diameter, and large-.0164 inch diameter. Two different spiral copper tubes were used. Tube 1 had five ridges with a distance of .3513 inches. Tube 2 had three ridges with .7069 inches between them.

The overall heat transfer coefficient, U_o, is defined in the following equation(18).

$$q = U_o A_o \overline{\Delta T}_L \qquad (1)$$

where,

q = heat loss, BTU/hr

U_o = overall heat transfer coefficient, BTU/hr-ft^2-^{o}F

A_o = outside surface area, ft^2

$\overline{\Delta T}_L$ = logarithmic mean temperature difference, ^oF

The outside surface area, A_o, for a twelve foot length of spiral tube was calculated as 5.15 square feet for Tube 1 and 4.02 square feet for Tube 2. The temperature of the fluidized bed, T_b, was constant throughout the bed. A difference of 1 ^oF was the largest deviation found in the three bed temperature readings after steady state was reached. The following equation was used for the logarithmic mean temperature difference.

$$\overline{\Delta T}_L = \frac{(T_b - T_i) - (T_b - T_o)}{\ln\left[\frac{T_b - T_i}{T_b - T_o}\right]} \qquad (2)$$

where,

$\overline{\Delta T}_L$ = logarithmic mean temperature difference, ^oF

T_b = bed temperature, ^oF

T_i = inlet water temperature, ^oF

T_o = outlet water temperature, ^oF

A steady state energy balance on the water in the spiral tube gives an equation for the heat lost from the water to the tube. The Reynolds number for the range of

water flow rates used in this study are in the turbulent region of flow, therefore, the inlet and outlet water temperatures should be nearly constant with respect to tube radius. The following equation is the result of the energy balance.

$$q = W_{H_2O}\, C_{pH_2O}\, (T_i - T_o) \qquad (3)$$

where,

q = heat loss, BTU/hr

W_{H_2O} = mass flow rate of water, lbs/hr

C_{pH_2O} = heat capacity of water, BTU/lb-^oF

T_i = inlet water temperature, ^oF

T_o = outlet water temperature, ^oF

Substituting equation (3) into equation (1) and solving for the overall heat transfer coefficient gives:

$$U_o = \frac{W_{H_2O}\, C_{pH_2O}\, (T_i - T_o)}{A_o\, \overline{\Delta T}_L} \qquad (4)$$

Using the two different spiral copper tubes and varying particle diameter and air mass velocity, data was collected. For each run, a value for U_o was calculated using equation (4). The results are given on Figure 7.

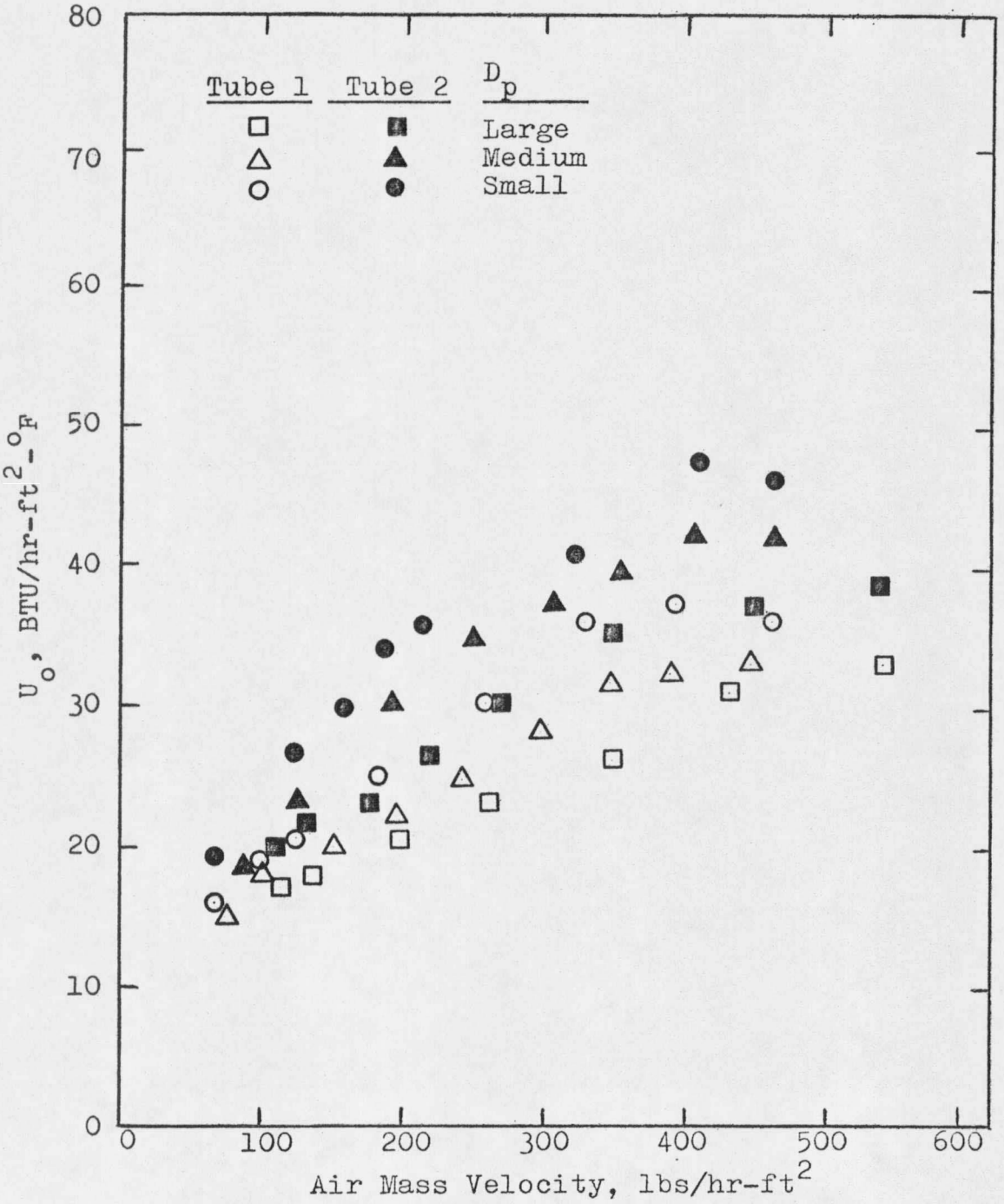

FIGURE 7. U_o VERSUS AIR MASS VELOCITY

The inlet water temperature was kept in the range of 190-196 ^{o}F. The bed temperature was always in the range of 148-166 ^{o}F, therefore, the effects of the changes in the fluidized bed properties are assumed negligible. Using the small glass beads, data was collected for each spiral tube throughout a large water flow range holding the other experimental variables constant. The following equation is the definition for the relationship between the overall heat transfer coefficient and the inside and outside heat transfer coefficients, neglecting the effect of fouling on the copper surface.

$$\frac{1}{U_o} = \frac{1}{h_o} + \frac{\Delta r\, D_o}{k\, \overline{D}_L} + \frac{A_o}{A_i\, h_i} \qquad (5)$$

where,

h_o = outside heat transfer coefficient, BTU/hr-ft^2-^{o}F

h_i = inside heat transfer coefficient, BTU/hr-ft^2-^{o}F

A_o = outside surface area, ft^2

A_i = inside surface area, ft^2

Δr = thickness of spiral tube, ft

k = thermal conductivity of spiral tube, BTU/hr-ft-^{o}F

D_o = outside diameter of spiral tube, ft

$\overline{D}_L$ = logarithmic mean diameter of spiral tube, ft

The effect of $\Delta r\ D_o/k\ \bar{D}_L$ was assumed negligible for copper tube. Using a Wilson plot analysis(19), the effect of $A_o/\ A_i\ h_i$ was found by plotting $1/U_o$ versus $(1/W_{H_2O})^{.8}$ For turbulent flow, the Nusselt number, Nu, is a function of the Reynolds number to the .8 power. The Reynolds number is directly proportional to the mass flow rate. The results of this analysis are shown on Figure 8. For both tubes, a straight line relationship fits the data for the range of water flow rates. Since the heat transfer properties of the fluidized bed do not depend on the water flow rate in the spiral tube, the following equation was used to account for the effect of water flow rate on the overall heat transfer coefficient.

$$\frac{A_o}{A_i\ h_i} = \frac{\text{slope}}{(W_{H_2O})^{.8}} \qquad (6)$$

From Figure 8, slope equals .484 for Tube 1 and slope equals .546 for Tube 2. Combining equation (5) and equation (6) and solving for h_o, the following relationship is obtained.

$$h_o = \frac{1}{\frac{1}{U_o} - \frac{\text{slope}}{(W_{H_2O})^{.8}}} \qquad (7)$$

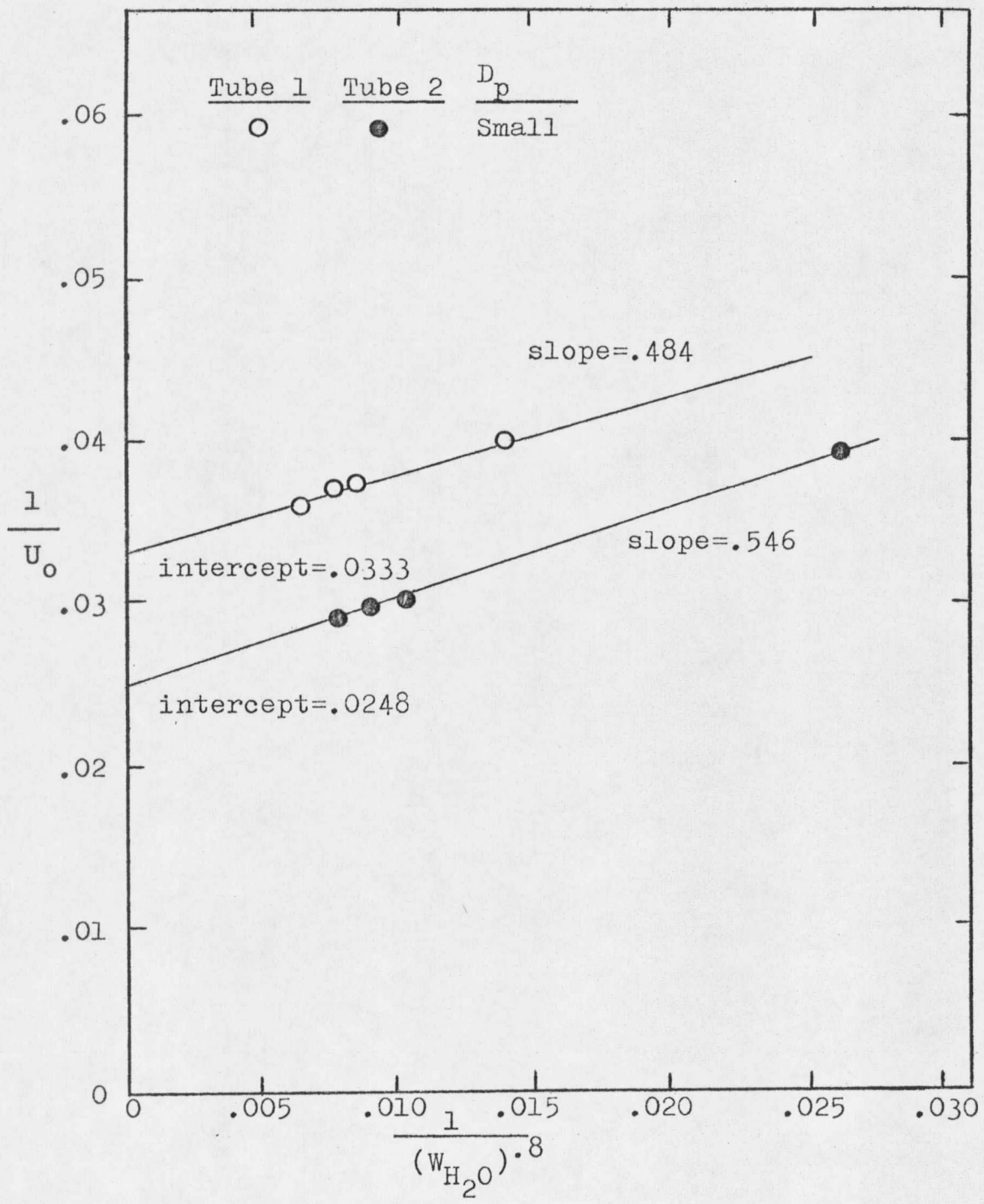

FIGURE 8. WILSON PLOT ANALYSIS

Using this equation, it is now possible to calculate the outside heat transfer coefficient, h_o, for all of the data collected. The results are shown on Figure 10. Figure 11 shows the results of h_o versus particle diameter for Tube 1 and Figure 12 for Tube 2. An increase in heat transfer coefficients for decreased particle size is clearly evident, approximately 35 per cent increase in coefficients for small particles to large particles.

Figure 13 and Figure 14 show the effect of h_o versus air mass velocity for the small and medium sized particles. The general shape of the curves of the relationship between the points is given in Figure 9. The curves are steepest

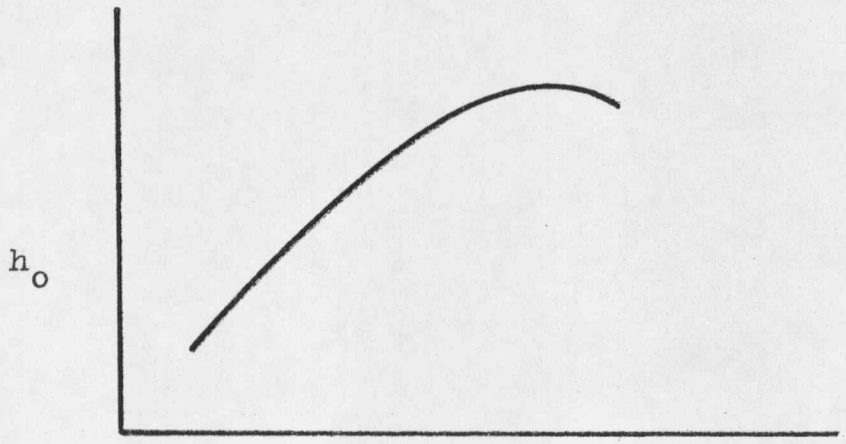

FIGURE 9. h_o VERSUS AIR MASS VELOCITY

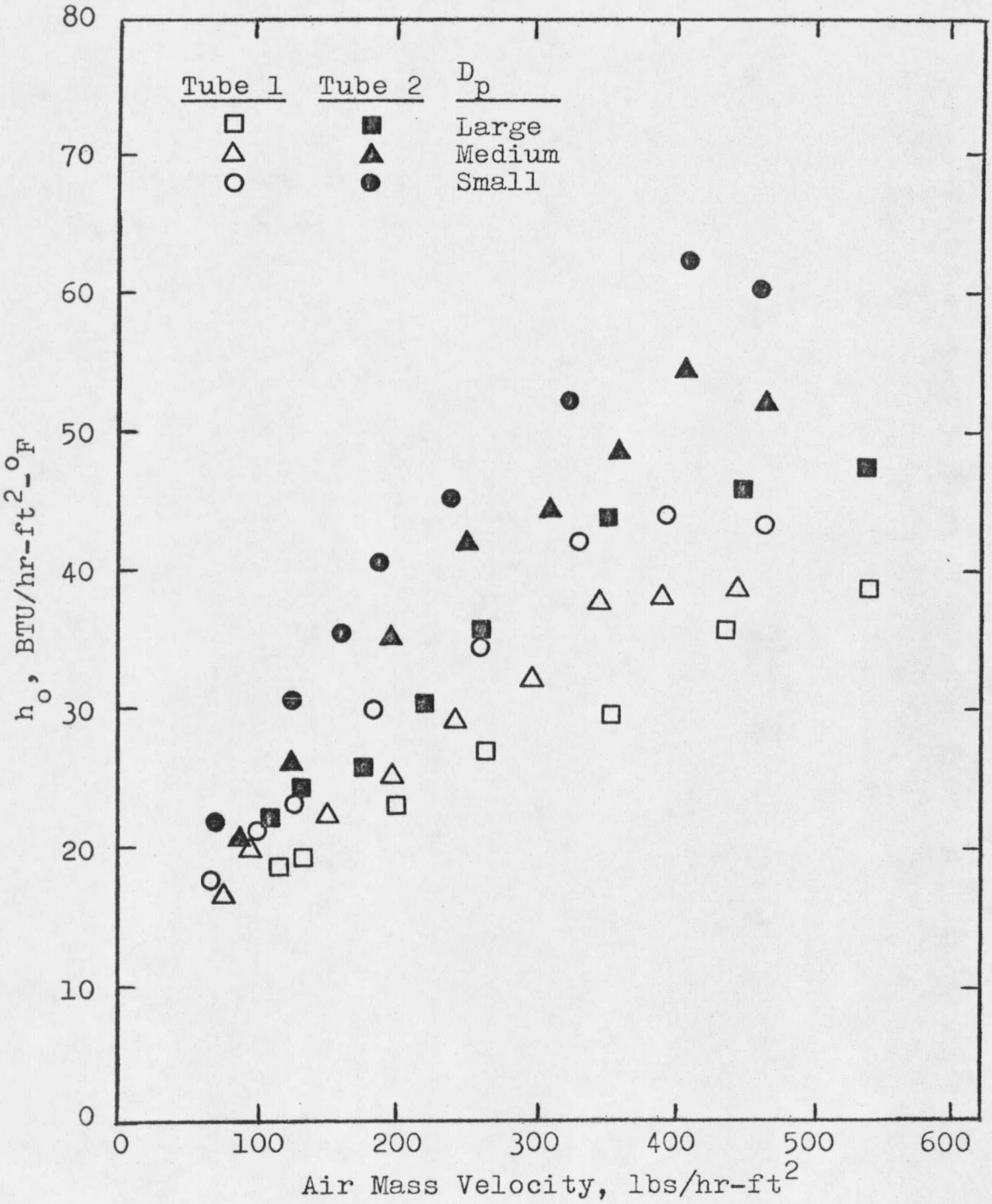

FIGURE 10. h_o VERSUS AIR MASS VELOCITY, ALL TUBES

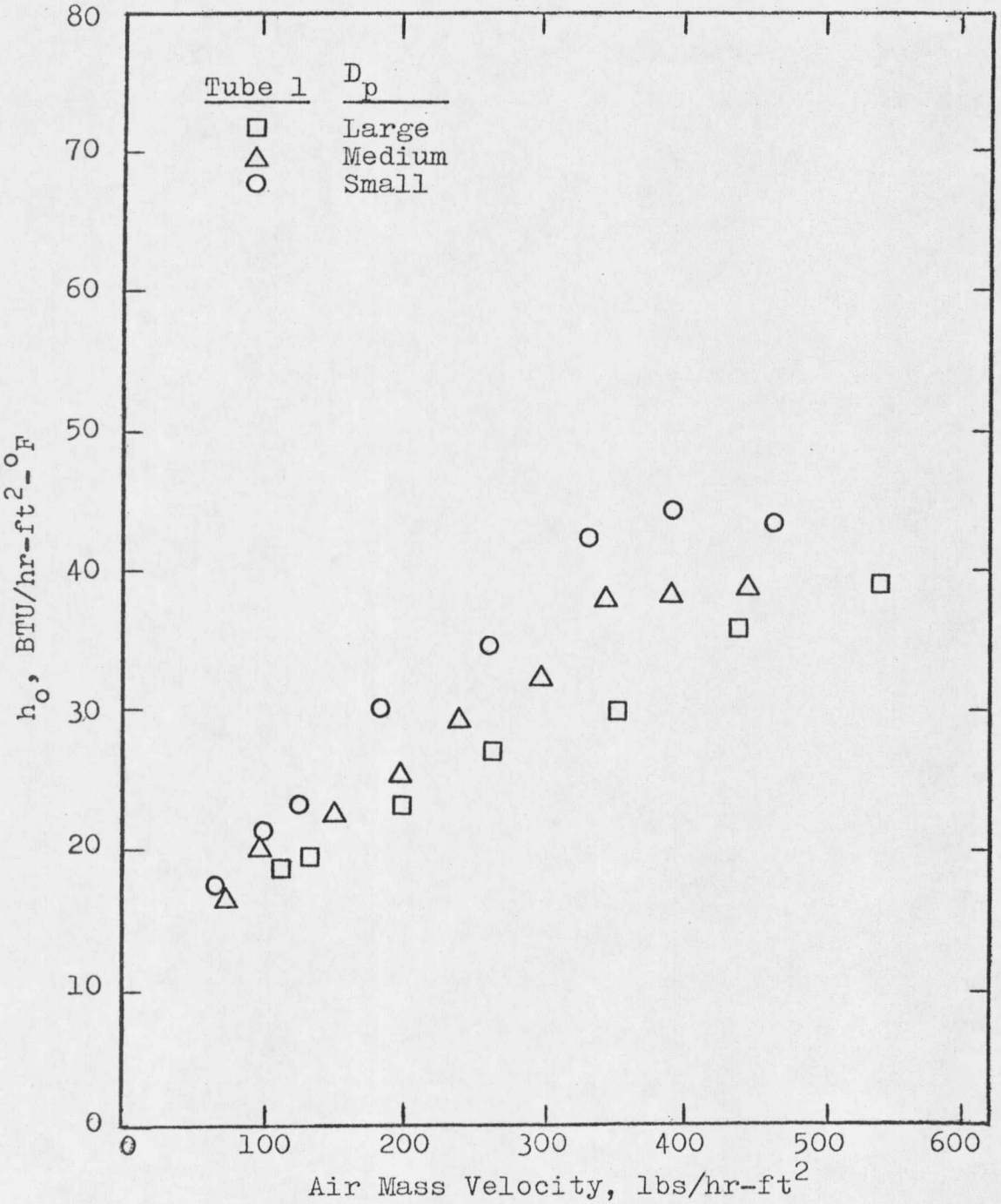

FIGURE 11. h_o VERSUS AIR MASS VELOCITY, TUBE 1

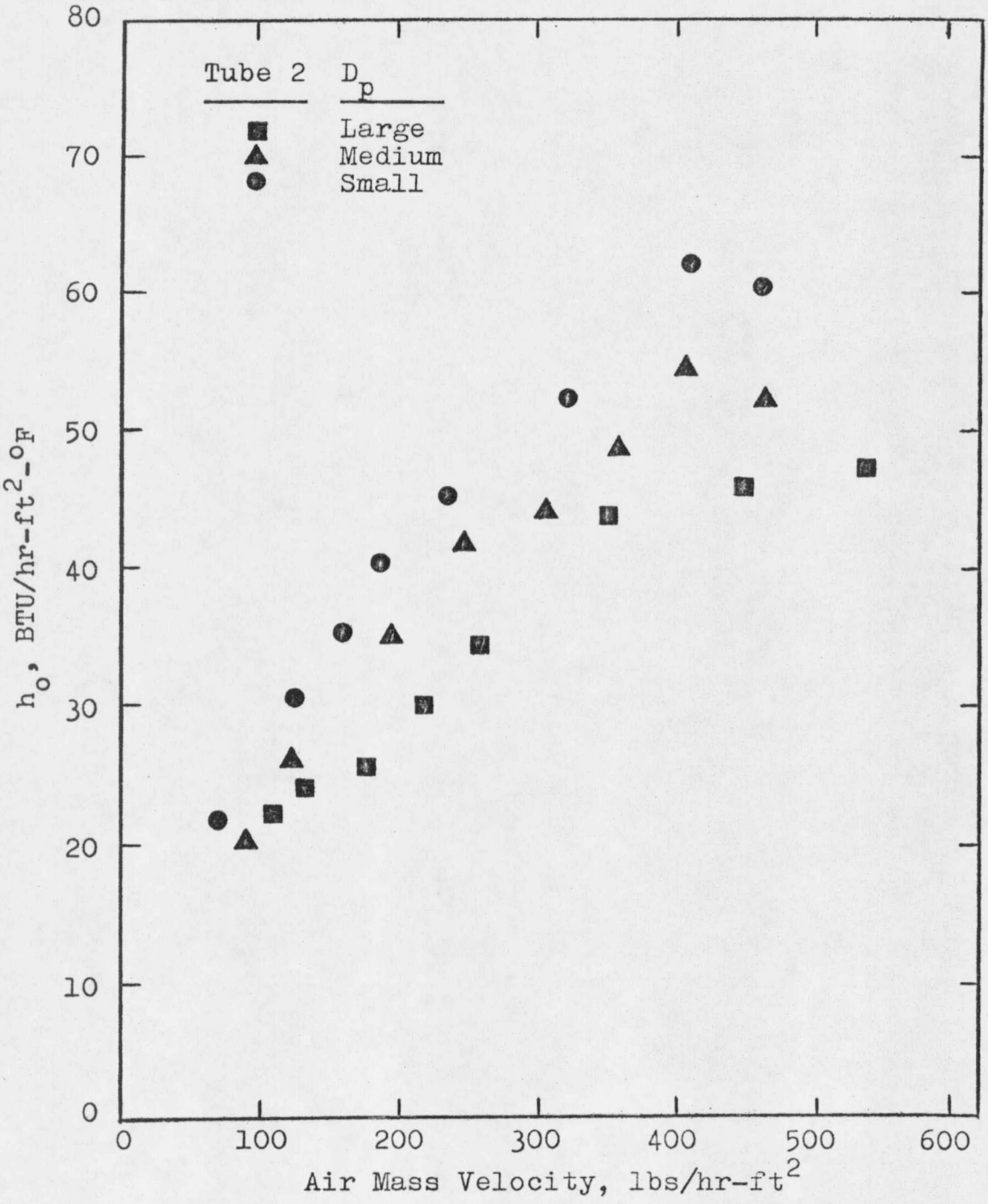

FIGURE 12. h_o VERSUS AIR MASS VELOCITY, TUBE 2

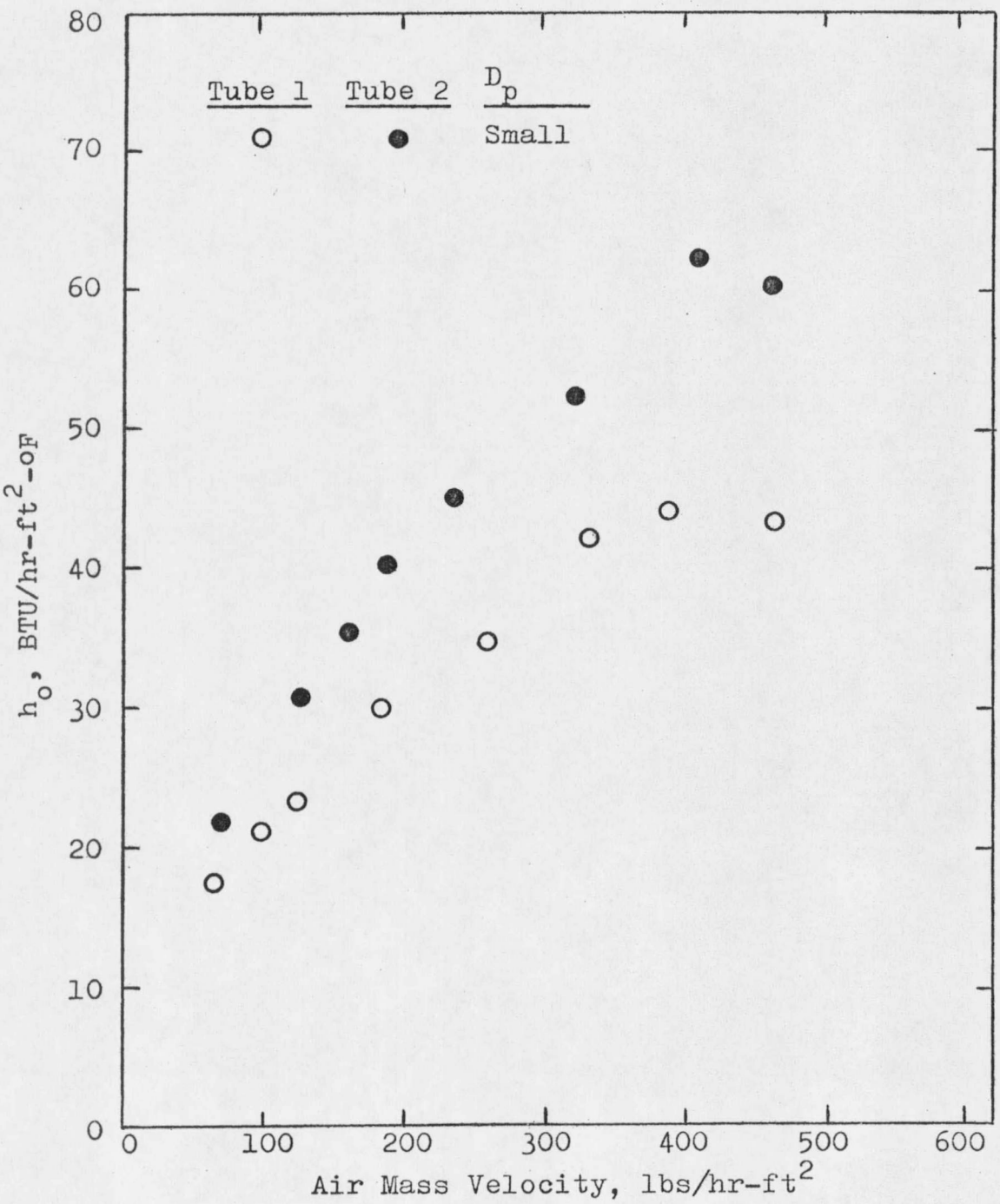

FIGURE 13. h_o VERSUS AIR MASS VELOCITY, SMALL PARTICLES

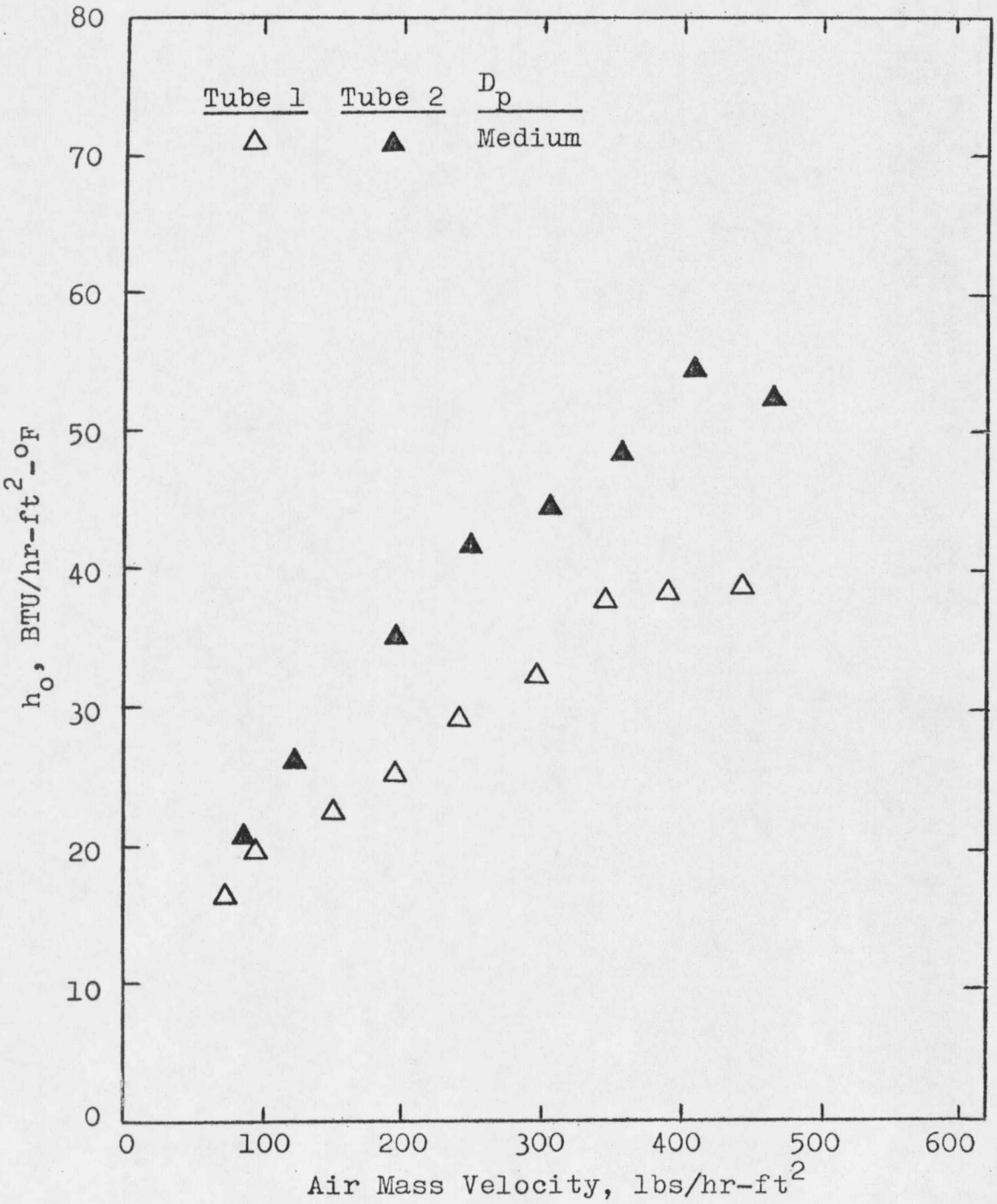

FIGURE 14. h_o VERSUS AIR MASS VELOCITY, MEDIUM PARTICLES

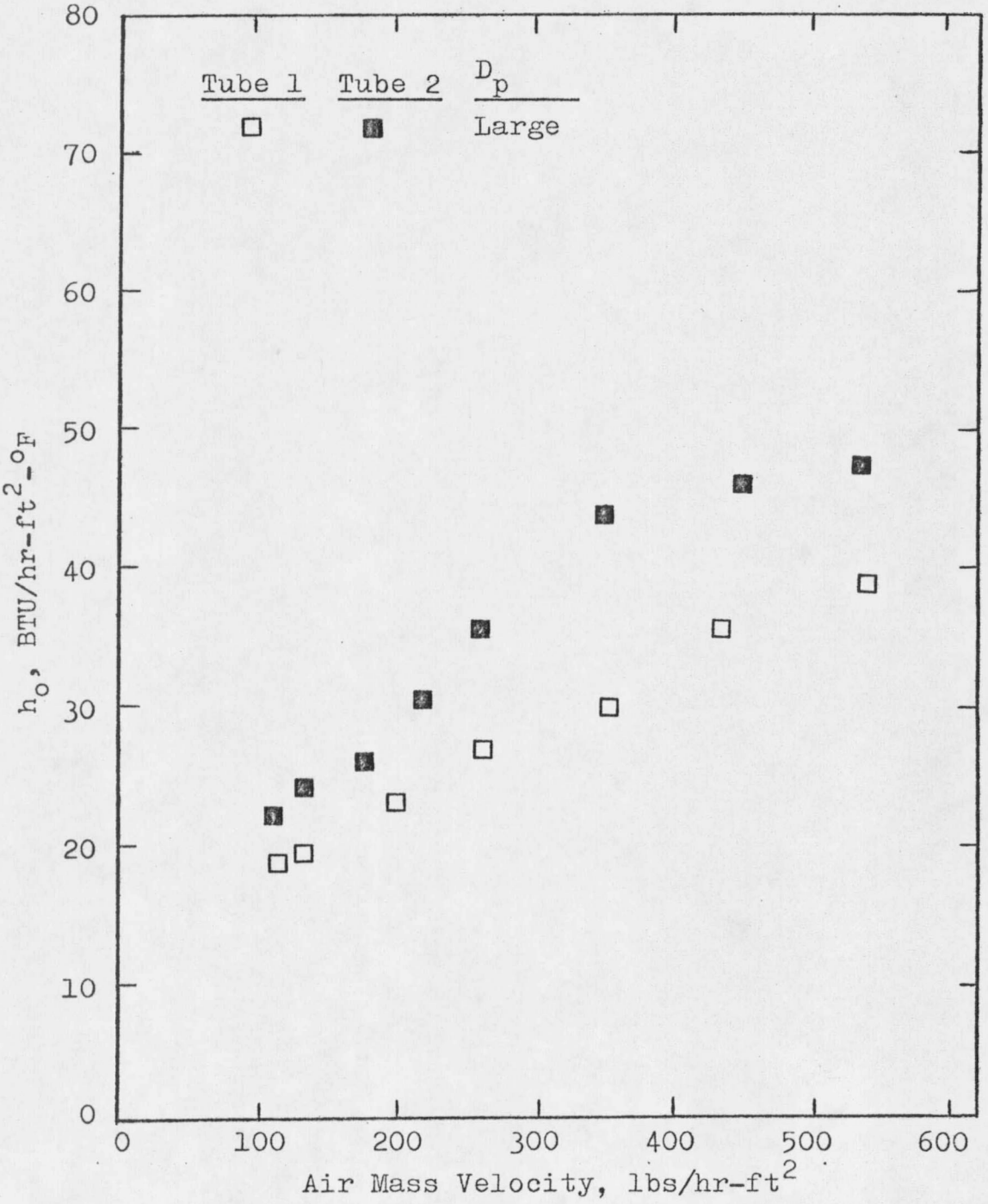

FIGURE 15. h_o VERSUS AIR MASS VELOCITY, LARGE PARTICLES

at air mass velocities near the minimum fluidization velocity and then level off and reach a maximum at higher flow rates. The particles were being blown to the top of the column at these higher air flow rates. This large expansion of the bed (less particles in the area around the coil in the bottom of the column) could explain the leveling and maximum heat transfer coefficients. The coefficients for the large particles, shown on Figure 15, increased with increasing air flow rate. A maximum or leveling did not occur in the air flow rate range in which the data was collected. This is explained by the less vigorous particle movement of the large particles at the same air mass velocity.

It is evident that the heat transfer coefficients for Tube 2 are higher than for Tube 1. For the small particles, this increase can be as high as 45 per cent. The reason for the lower coefficients for Tube 1 could be that the distance between ridges is small for this particle range. In other research work done with helical copper finned tubes(17), a spacing of less than 30 particle diameters between fins caused a reduced heat transfer coefficient. The distance between ridges for Tube 1 is .3513 inches and .7069 inches for Tube 2. For the large

particles, .0164 inch diameter, 30 particle diameters is .492 inches. Therefore, the spacing of the ridges is an explanation for decreasing coefficients from Tube 2 to Tube 1. The distance between the ridges narrows as the groove approaches the center of the tube on the tube with 5 ridges. This is due to the method of spiraling the tubing. The width of the bottom of the groove is much less than the distance between ridges calculated at the outside diameter. The reason for reduced heat transfer coefficients is probably due to an obstruction of particle movement.

Another reason for this effect could be nonuniform temperature distribution of the water in the outside edge of each ridge. The ridges on Tube 1 are pinched closer than on Tube 2. If the water at these extreme points is much cooler than the average water temperature in the tube at a certain point along the length of the tube, there will be less temperature difference to drive heat to the bed.

High rates of heat transfer to cooling tubes are necessary for fluidized combustors having high heat generation rates. Chen and Withers(14,15) have proposed the following ratio as a figure of merit,

$$\frac{(h\,A)_{\text{finned tube}}}{(h\,A)_{\text{plain tube}}}$$

where, $(h\,A)_{\text{plain tube}}$ is the heat transfer coefficient times surface area for a plain tube of a diameter equal to the tip diameter of the finned tube operating at the same bed conditions. This is a conservative estimate of heat transfer duty per unit bed volume for extended surface versus plain tubes.

From the definition of the heat transfer coefficient,

$$q = h\,A\,\Delta T \qquad (9)$$

rearranging,

$$q/\Delta T = h\,A \qquad (10)$$

the figure of merit can now be rewritten and applied to spiral tubing.

$$\frac{(q/\Delta T)_{\text{spiral tube}}}{(q/\Delta T)_{\text{plain tube}}}$$

Figure 16 shows the results of this comparison for spiral copper tubes. The above ratio is plotted as a

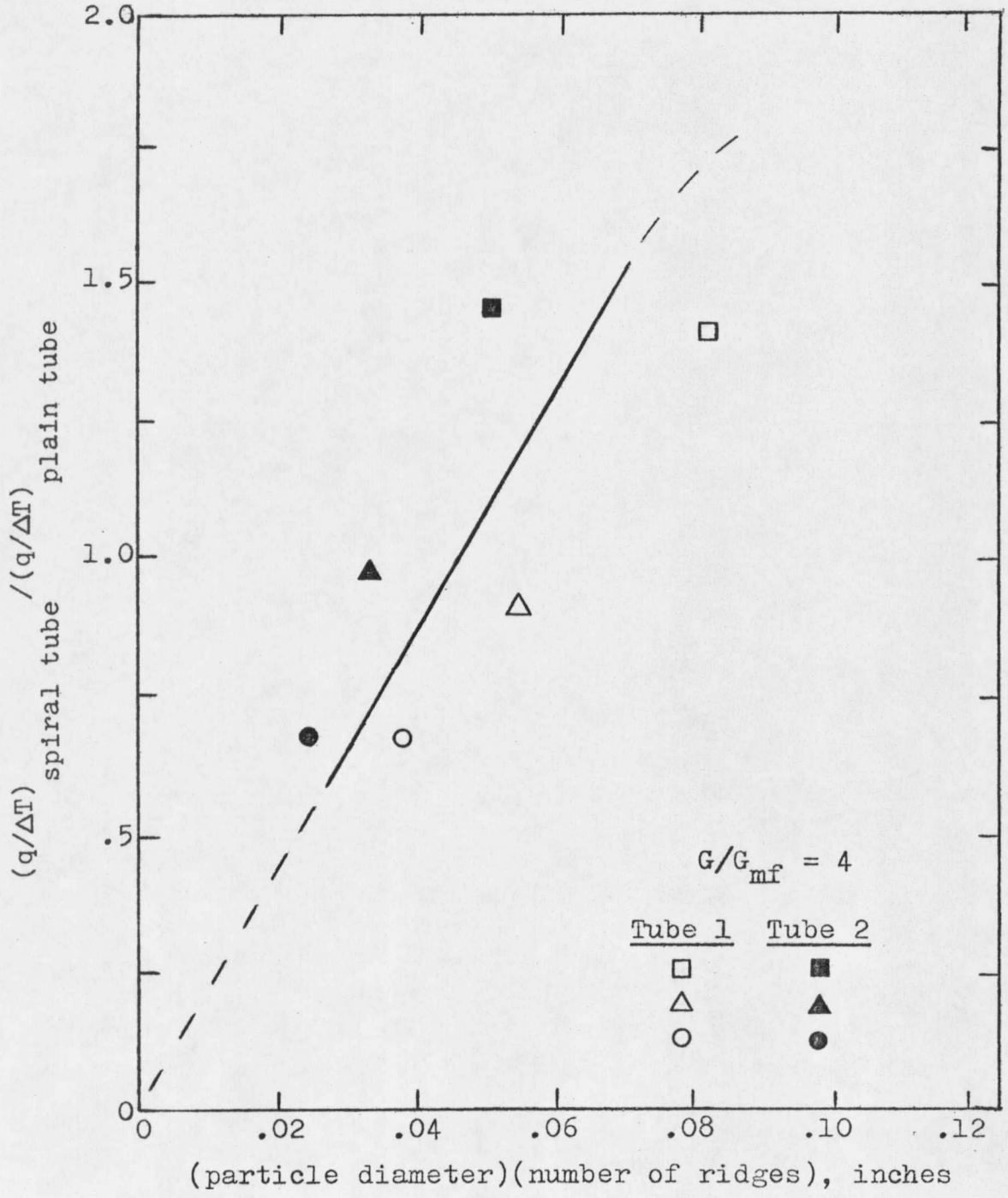

FIGURE 16. PERFORMANCE OF SPIRAL TUBES

function of particle diameter times the number of ridges on the spiral tube. The data has been calculated for G/G_{mf} equal to 4 at all points. The Vreedenberg correlation for bare tubes(11) was used to calculate a value for $(hA)_{plain\ tube}$. This correlation is given in the calculation section. It has a variable for differences in outside diameter of bare tubes in a fluidized bed. The coiled tube should not have exactly the same coefficients as a horizontal tube. The surface area, A, for a plain tube was calculated for a twelve foot length of 1-1/8 inch outside diameter tube. It is evident that the performance increases as the particle diameter times the number of ridges increases. For the same particle size, the performance as a function of a change in the number of ridges on the spiral tube is constant in this range. For the individual tubes, the performance is highest for the large particles and decreases for the medium and small particles. There should be a point where the performance begins to decrease sharply as the distance between the ridges decreases (an increase in the number of ridges or a larger pitch) or an increase in particle size. This due to a decrease in particle mobility in the groove between the ridges. It is recommended that a coil of 1-1/8 inch outside diameter

copper tube of the same gauge and length be studied at these air mass velocities to have a more realistic comparative performance of the spiral tubes. The coiled tube is close to a horizontal tube, but may have some of the performance characteristics of a vertical tube.

Bartel and Genetti(15) and Priebe and Genetti(16) showed gains as great as 80 per cent compared to plain tubes using horizontal serrated carbon steel tubes. Priebe and Genetti(16) showed gains up to 60 per cent for horizontal copper spined tubes. Kratovil(17) observed gains as large as 190 per cent for horizontal helical copper finned tubes. Using this method of comparing tubes with increased surface area to plain tubes, these tubes exceed the performance of the spiral copper tubes. Lack of data for plain tubes for this bed geometry and coil configuration leaves some doubt about the comparative performance.

Keairns(20) indicated that caps of stagnant particles form on the top of horizontal tubes in a fluidized bed, causing a decrease in the heat transfer coefficients in this region. Bartel and Genetti(15) found little effect due to tube spacing when adjacent tube surfaces were 1-1/2 inches or more apart. Since the spacing of the coil

turns on both spiral copper tubes used in this study was more than two inches, this effect should not be a consideration in the performance of the spiral tubes.

CORRELATION

The experimental data collected from the two different spiral tubes at varying particle diameter and air flow rate were correlated into an equation. The particle mode heat transfer model presented by Ziegler, Koppel, and Brazelton (9) and extended by Genetti and Knudsen(10) was used to correlate the experimental data. From the particle mode heat transfer model, the following equation describes the rate of heat transfer from a surface in a fluidized bed.

$$Nu_p = \frac{h_o D_p}{k_g} = \frac{7.2}{\left[1 + \frac{6 k_g \bar{\theta}}{\rho_s C_{ps} D_p^2}\right]^2}$$

where,

Nu_p = particle Nusselt number, dimensionless

h_o = heat transfer coefficient, BTU/hr-ft^2-^{o}F

D_p = particle diameter, ft

k_g = thermal conductivity of fluidizing medium, BTU/ft-hr-^{o}F

$\bar{\theta}$ = average contact time, hr

ρ_s = density of solid particles, lbs/ft^3

C_{ps} = heat capacity of solid particles, BTU/lb-^{o}F

The value of 7.2 could be replaced by $10(1-\epsilon)^{.5}$ as

suggested by Genetti and Knudsen. The particle fraction, $(1-\epsilon)$, can be calculated for each run. This value did not have a large range of variation for the different air flow rates and an average value of $10(1-\epsilon)^{.5}$ equals 7.26 was calculated for the correlation. This agrees within 1 per cent of the 7.2 value. The particles were of the same material, therefore, the heat capacity and density were constant. Particle residence time at the surface, $\bar{\theta}$, was not measured directly, but it is a function of tube geometry, particle diameter, and air flow rate. The following form for correlating the particle Nusselt number can be written using dimensionless analysis to introduce dimensionless groups in place of $\bar{\theta}/D_p^2$.

$$Nu_p = \frac{7.26}{\left[1 + C_1\left(\frac{G}{G_{mf}}\right)^a\left(\frac{D_p}{L}\right)^b\left(S\right)^c\right]^2}$$

where,

Nu_p = particle Nusselt number, dimensionless

G = air mass velocity, lb/hr-ft^2

G_{mf} = minimum fluidization velocity, lb/hr-ft^2

D_p = particle diameter, inches

L = distance between ridges on spiral tube, inches

S = number of ridges on spiral tube, dimensionless

The physical properties were evaluated at the bed temperature. The minimum fluidization velocity, G_{mf}, was calculated using the Leva correlation(5), which agreed within 5 per cent of the experimental data. Functions must now be found for a, b, c, and C_1 using the data from this investigation.

Since G/G_{mf} had a larger number of different values than the other dimensionless groups, a value for a is obtained by rearranging the previous equation and taking the logarithm of both sides.

$$\log (7.26/Nu_p)^{.5}-1 = a \log(G/G_{mf}) + \log C_1(D_p/L)^b S^c$$

From a graph of $\log (7.26/Nu_p)^{.5}-1$ plotted versus $\log(G/G_{mf})$, six straight lines were made using a linear regression analysis. The slopes of these lines are the a values and the intercepts are the $\log C_1(D_p/L)^b S^c$ values.

It was assumed a is a function of D_p/L and S.

$$a = f(D_p/L, S) = C_2 (D_p/L)^d S^e$$

Multiplying both sides by -1 and taking the logarithm:

$$\log(-a) = d \log(D_p/L) + \log(-C_2 S^e)$$

From a graph of $\log(-a)$ plotted versus $\log(D_p/L)$, two straight lines using a linear regression analysis

were obtained for constant values of S(3,5). The slopes of these two lines are the d values. Assuming a straight line relationship between the two points plotted on a graph of d versus S, the following equation is obtained:

$$d = -.0428\ S + .540$$

The intercepts, I_1, of the two lines are the values for $\log(-C_2 S^e)$, therefore,

$$I_1 = e \log S + \log(-C_2)$$

A graph of I_1 versus log S was made and a straight line relationship between the two points is assumed. The slope of this line, -1.69, is equal to e. The antilogarithm of the intercept, -21.9, is the value of C_2.

The value for a is now equal to the following:

$$a = -21.9\ (D_p/L)^{-.0428S+.540}\ S^{-1.69}$$

The intercepts, I_2, of the $\log\ (7.26/Nu_p)^{.5}-1$ versus $\log(G/G_{mf})$ graph are equal to $\log C_1 (D_p/L)^b S^c$, which can be expanded to the following:

$$I_2 = b \log(D_p/L) + \log(C_1 S^c)$$

A graph of I_2 versus $\log(D_p/L)$ was plotted and two straight

lines were drawn through the three points for both values of S using a linear regression analysis.

The slopes of the two lines from the graph are the b values, and the intercepts are the values of $\log(C_1 S^c)$. It was assumed that b is a function of the number of ridges, S, which can be written:

$$b = C_3 S^f$$

Taking the logarithm of both sides, multiplying by -1, and expanding:

$$\log(-b) = f \log S + \log(-C_3)$$

A straight line was drawn through the two points on the graph of log(-b) versus log S. The slope of this line, -.173, is equal to f. Taking the antilogarithm of the intercept, a value of -1.72 is obtained for C_3.

The intercepts, I_3, of the b sloped lines are values of $\log(C_1 S^c)$, when expanding gives:

$$I_3 = c \log S + \log C_1$$

Drawing a straight line between the two values for I_3 plotted versus log S, the slope, 2.87, is equal to c and the antilogarithm of the intercept, .000235, is equal

to C_1.

The final correlation is formed using the previously determined values.

$$Nu_p = \frac{7.26}{\left[1+.000235(G/G_{mf})^{-21.9(D_p/L)^{-.0428S+.540_S-1.69}} (D_p/L)^{-1.72}\, S^{-.173}\,(S)^{2.87}\right]^2}$$

where,

$Nu_p = h_o\, D_p/k_g$ = particle Nusselt number, dimensionless

h_o = heat transfer coefficient, BTU/hr-ft^2-^{o}F

D_p = particle diameter, ft

k_g = thermal conductivity of fluidizing medium, BTU/ft-hr-^{o}F

G = air mass velocity, lbs/hr-ft^2

G_{mf} = minimum fluidization velocity, lbs/hr-ft^2

L = distance between ridges on spiral tube, ft

S = number of ridges on spiral tube, dimensionless

The values for the physical properties are evaluated at the bed temperature.

The data from all of the experimental runs was plotted on log-log paper, $Nu_p/7.26$ versus $[\quad]^2$ as shown on

Figure 17. It can be seen on this figure, which has a slope of a -1, that the experimental data fit the correlation equation to within plus or minus 15 per cent.

Table 3 gives the range of experimental variables over which this correlation applies.

Table 3. Range of Correlation

Variable	Range
Particle diameter, D_p	.0076, .0109, and .0164 inch
Fluidizing velocity, G	60 to 560 lbs/hr-ft^2
Number of ridges, S	3,5
Distance between ridges, L	.3513, .7069 inch
Bed temperature, T_b	148^{o}F to 166^{o}F
Tube diameter, D_t	1-1/8 inch

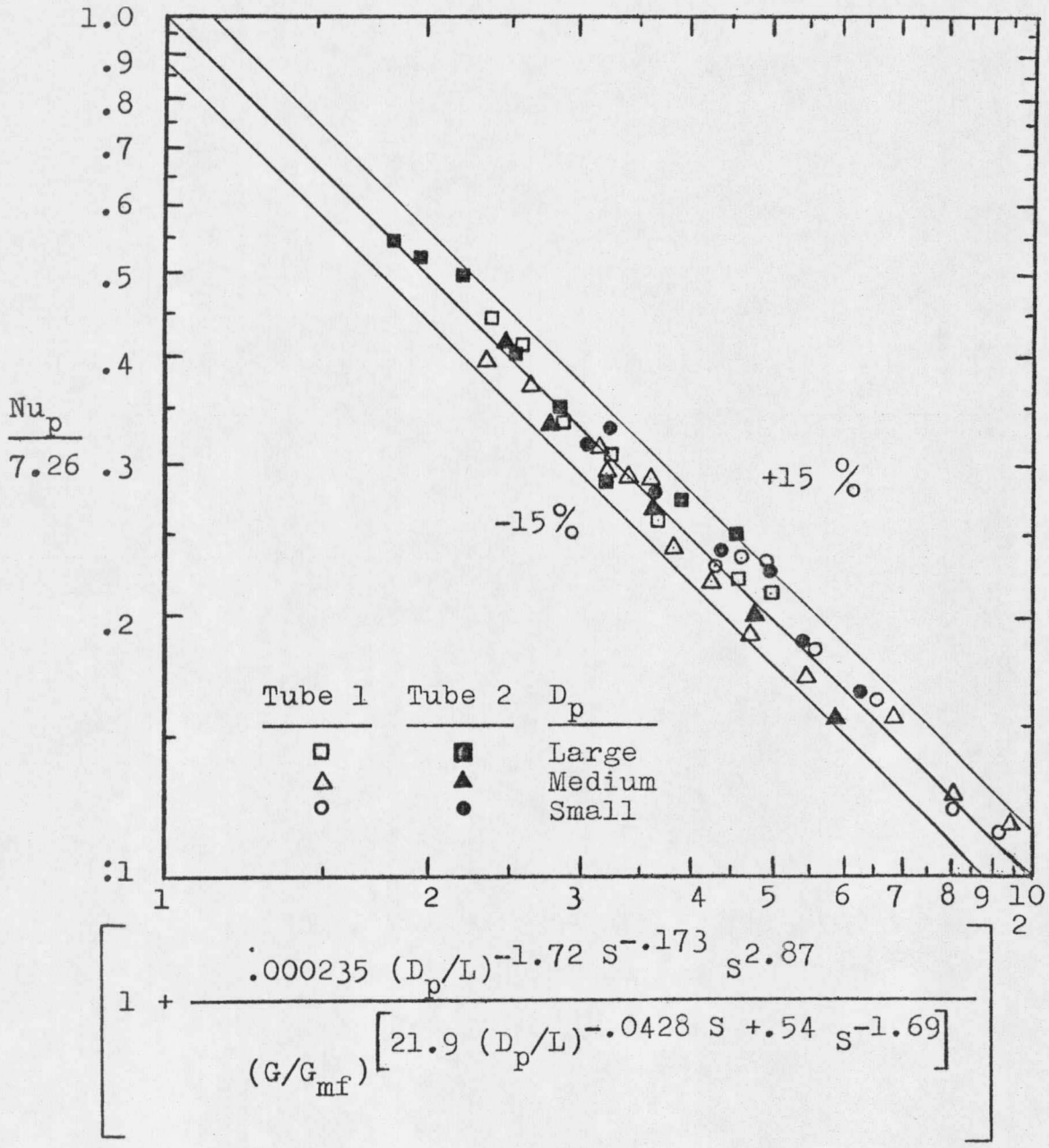

FIGURE 17. CORRELATION FOR SPIRAL TUBES

ERROR ANALYSIS

Assuming U_o is only effected by the experimental determinations of q and $(T_w - T_b)$, the error analysis is performed on the following equation.

$$U_o = \frac{W_{H_2O}\, C_{pH_2O}\, \ln \dfrac{T_i - T_b}{T_o - T_b}}{A_o}$$

The measurement of the water flow rate is assumed accurate to 5 lbs/hr. No error is assumed in determining the tube surface area and the heat capacity of water. A minimum value of $\ln(T_i - T_b \,/\, T_o - T_b)$ of .22 was experimentally observed. This occurred at the lowest value of U_o, which was encountered at the lower limit of the range of air mass velocity. Since it is the smallest value of U_o, the experimental error is at the maximum effect. The thermocouple readings are assumed accurate to $\pm$ .5°F, however, for several runs fluctuations in steam pressure to the heat exchanger caused large fluctuations in inlet water temperature.

Using the above experimental accuracies, maximum and minimum errors for U_o are determined.

Maximum U_o

$$U_{oMAX} = \frac{(W_{H_2O}+5)(C_{pH_2O}) \ln \frac{T_i+.5 - T_b+.5}{T_o-.5 - T_b+.5}}{A_o}$$

$$\text{Error} = \frac{(U_{oMAX} - U_o)}{U_o} \times 100 = +13.1$$

Minimum U_o

$$U_{oMIN} = \frac{(W_{H_2O}-5)(C_{pH_2O}) \ln \frac{T_i-.5 - T_b-.5}{T_o+.5 - T_b-.5}}{A_o}$$

$$\text{Error} = \frac{(U_{oMIN} - U_o)}{U_o} \times 100 = -27.2$$

Since this is the lowest heat transfer coefficient value encountered, the maximum error should be $\pm$ 20 per cent.

CALCULATIONS

Air Mass Velocity

A vena contracta orifice with a water filled manometer were used to measure the air flow rates in the column. The following equation was used for the calculations(1).

$$G = \frac{3600\ C_o\ Y\ S_c}{A_c} \sqrt{\frac{2\ g_c\ (P_1-P_2)\ \rho_1}{1-\beta^4}}\ ,\ \text{lbs/hr-ft}^2$$

where,

G = air mass velocity, lbs/hr-ft^2

C_o = orifice coefficient, dimensionless

Y = expansion factor, dimensionless

S_c = cross sectional area of orifice, ft^2

A_c = cross sectional area of column, ft^2

g_c = gravitational constant, ft-lb$_m$/hr^2-lb$_f$

P_1 = pressure at upstream pressure tap, lb$_f$/ft^2

P_2 = pressure at downstream pressure tap, lb$_f$/ft^2

ρ_1 = density of air at the upstream pressure, lb$_m$/ft^3

β = ratio of orifice diameter to inside pipe diameter, dimensionless

For a square edged orifice, the expansion factor is given as follows:

$$Y = 1 - \frac{P_1 - P_2}{P_1 K_r} (.41 - .35\beta^4)$$

where,

$$K_r = C_p/C_v$$

The orifice coefficient is a function of the Reynolds number. It was found to be nearly constant at .61 for the range of air flow rates used.

Temperature

The temperatures were read directly using thermocouples connected to a Honeywell chart recorder.

Bed Temperature

The value used for the bed temperature, T_b, was the average of the three bed thermocouple readings.

Water Mass Velocity

The water mass velocity, W_{H_2O}, was measured by weighing the amount of water discharged over a given time period.

Surface Area of the Spiral Tube

The surface area of each tube, A_o, was determined by

measuring the reduced length of the tube compared to a bare tube of the same diameter.

Air Thermal Conductivity

Air thermal conductivity, k_g, was determined by linear interpolation between selected list values in Kreith(19). Evaluation temperature was the bed temperature, T_b, and the units are BTU/hr-ft-^oF.

Air Viscosity

Air viscosity was calculated for each bed temperature from the following equation which was fit to experimental data.

$$\mu_g = (2.45(T_b-32) + 1538.1)\ 2.688X10^{-5}\ , \text{ lb/ft-hr}$$

where,

μ_g = air viscosity, lb/ft-hr

T_b = bed temperature, ^oF

Particle Reynolds Number

$$Re_p = \frac{G\ D_p}{\mu_g}\ , \text{ dimensionless}$$

where,

G = air mass velocity, lbs/hr-ft^2

D_p = particle diameter, ft

μ_g = air viscosity evaluated at bed temperature, lbs/hr-ft

Overall Heat Transfer Coefficient

The following equation for the overall heat transfer coefficient was derived in the previous material.

$$U_o = \frac{W_{H_2O}\, C_{pH_2O}\, \ln \frac{T_i - T_b}{T_o - T_b}}{A_o}, \quad \text{BTU/hr-ft}^2\text{-}^\circ\text{F}$$

where,

C_{pH_2O} = heat capacity of water, BTU/lb-$^\circ$F

W_{H_2O} = water mass velocity, lbs/hr

T_i = inlet water temperature, $^\circ$F

T_o = outlet water temperature, $^\circ$F

T_b = bed temperature, $^\circ$F

A_o = outside surface of spiral tube, ft^2

Outside Heat Transfer Coefficient

The outside heat transfer coefficient, h_o, is calculated

from the following equation derived in the previous material.

$$h_o = \frac{1}{\frac{1}{U_o} - C_4 (1/ W_{H_2O})^{.8}} , \quad BTU/hr\text{-}ft^2\text{-}^oF$$

where,

U_o = overall heat transfer coefficient, $BTU/hr\text{-}ft^2\text{-}^oF$

W_{H_2O} = water mass velocity, lbs/hr

The term $C_4(1/W_{H_2O})^{.8}$ was determined for each tube from a Wilson plot analysis which relates the water mass velocity to the inside heat transfer coefficient.

Particle Nusselt Number

$$Nu_p = \frac{h_o D_p}{k_g} , \quad \text{dimensionless}$$

where,

h_o = outside heat transfer coefficient, $BTU/hr\text{-}ft^2\text{-}^oF$

D_p = particle diameter, ft

k_g = thermal conductivity of fluidizing air at bed temperature, $BTU/hr\text{-}ft\text{-}^oF$

Particle Fraction

$$1-\epsilon = \frac{\Delta P}{L_t\ (\rho_s - \rho_g)} \quad , \quad \text{dimensionless}$$

where,

$1-\epsilon$ = particle fraction, dimensionless

ΔP = pressure drop across the bed, lbs/ft^2

L_t = distance between pressure taps, ft

ρ_s = density of particles, lbs/ft^3

ρ_g = density of fluidizing air, lbs/ft^3

Minimum Fluidization Velocity

The values of minimum fluidization velocity, G_{mf}, used in the correlation of the data for this investigation is calculated from the Leva correlation(5).

$$G_{mf} = \frac{688\ D_p^{1.82} \rho_g (\rho_s - \rho_g)^{.94}}{\mu_g^{.88}} \quad , \quad \text{lbs/hr-ft}^2$$

where,

D_p = particle diameter, ft

ρ_g = density of fluidizing medium at bed temperature, lbs/ft^3

ρ_s = density of bed particles, lbs/ft^3

μ_g = dynamic viscosity of fluidizing medium at bed temperature, centipoise

Heat Transfer Coefficient of Plain Tube

The value for $h_{plain\ tube}$ which was used in comparing the data from this study to a plain tube was calculated from the following correlation by Vreedenberg(11).

$$\frac{h\ D_t/k_g}{(C_{ps}\ \mu_g/k_g)^{.3}} = 420\left(\frac{G\ D_t\ \rho_s}{\rho_g\ \mu_g}\ x\ \frac{\mu_g^2}{D_p^3\ \rho_s^2\ g}\right)^{.3}$$

where,

h =heat transfer coefficient, BTU/hr-ft^2-^{o}F

D_t = outer tube diameter, ft

k_g = thermal conductivity of fluidizing medium at bed temperature, BTU/hr-ft-^{o}F

C_{ps} = heat capacity of particles at bed temperature, BTU/lb-^{o}F

μ_g = dynamic viscosity of fluidizing medium at bed temperature, lbs/ft-hr

ρ_g = density of fluidizing medium at bed temperature, lbs/ft^3

ρ_s = density of particles, lbs/ft^3

g = acceleration of gravity, ft/hr^2

CONCLUSIONS

There are several conclusions that may be drawn as a result of this investigation.

The fluidized bed heat transfer coefficients were inversely proportional to the particle diameter. A 35 per cent increase in heat transfer coefficients from the large particles (.0164 inches mean diameter) to the small particles (.0076 inches mean diameter).

The heat transfer coefficients increased as the air mass velocity was increased. For the small and medium sized particles, the transfer coefficients increased up to a certain rate where a maximum was reached. The range of air mass velocity was not sufficient to find a maximum or leveling of heat transfer coefficients for the large particles.

The spiral tube with three ridges had higher heat transfer coefficients than the tube with five ridges, up to 45 per cent increase. The comparative performance of the two spiral tubes was similiar for the range of particle diameter. Improved performance of 45 percent compared to bare tubes was found for the large diameter particles.

A correlation using the particle mode heat transfer model was formulated. This included variables for air

mass velocity, particle diameter, number of ridges and distance between the ridges on the spiral tube. The maximum deviation of 15 per cent from the correlation for the calculated heat transfer coefficients was within the range of experimental error.

RECOMMENDATIONS

The purpose of this type of research is to develop a general correlation for industrial fluidized bed applications. This must include a wide range of parameters. The scope of this type of correlation is much greater than one investigation can include.

The use of spiral tubing in fluidized beds appears to be encouraging because of performance, ease of handling, and conforming to cylindrical bed geometries. More work should be done with spiral tubes of varying outside diameter and ridge spacing (a function of pitch and the number of ridges).

There is some doubt as to the accuracy of using a horizontal bare tube correlation from other research for comparing performance of spiral tubes in a coil configuration. Further research using this bed geometry, particle size and material, and operating conditions is recommended for a coiled bare copper tube.

NOMENCLATURE

Symbol	Definition	Dimension
$a,b,c,d,e,f,C_1,C_2,C_3,I_1,I_2,I_3$	functions of experimental variables in correlation equation	dimensionless
A	surface area	ft^2
A_c	cross sectional area of column	ft^2
A_i	inside tube surface area	ft^2
A_o	outside tube surface area	ft^2
C_o	orifice coefficient	dimensionless
C_4	function of spiral tube in Wilson plot analysis	dimensionless
C_p	heat capacity at constant pressure	BTU/lb-^oF
C_{ps}	heat capacity of solid particles	BTU/lb-^oF
C_v	heat capacity at constant volume	BTU/lb-^oF
D_o	outside diameter of tube	inches
$\overline{D}_L$	logarithmic mean diameter of tube	inches
D_p	particle diameter	inches
D_t	outside tube diameter	inches
g	acceleration of gravity	ft/hr^2
G	air mass velocity	$lbs/hr-ft^2$
g_c	gravitational constant	$ft-lb/hr^2-lb_f$

Symbol	Definition	Dimension
G_{mf}	minimum fluidization velocity	lbs/hr-ft^2
h	heat transfer coefficient	BTU/hr-ft^2-^oF
h_i	inside heat transfer coefficient	BTU/hr-ft^2-^oF
h_o	outside heat transfer coefficient	BTU/hr-ft^2-^oF
k	thermal conductivity	BTU/hr-ft-^oF
k_g	thermal conductivity of fluidizing medium	BTU/hr-ft-^oF
K_r	ratio of C_p/C_v	dimensionless
L	distance between ridges on spiral tube	inches
L_t	distance between pressure taps	feet
Nu_p	particle Nusselt number	dimensionless
P_1	upstream pressure	lb_f/ft^2
P_2	downstream pressure	lb_f/ft^2
ΔP	pressure drop across the bed	lb_f/ft^2
q	rate of heat transfer	BTU/hr
r	radius	inches
Re_p	particle Reynolds number	dimensionless
Δr	tube wall thickness	inches
S	number of ridges on the spiral tube	dimensionless

Symbol	Definition	Dimension
S_c	cross sectional area of the orifice	ft^2
T_b	bulk bed temperature	^oF
T_f	fluid temperature	^oF
T_i	inlet water temperature	^oF
T_o	outlet water temperature	^oF
T_p	particle temperature	^oF
T_w	surface temperature	^oF
$T(r,\theta)$	unsteady state particle temperature	^oF
ΔT	temperature difference	^oF
$\overline{\Delta T}_L$	logarithmic mean temperature difference	^oF
U_o	overall heat transfer coefficient	BTU/hr-ft^2-^oF
W_{H_2O}	water mass velocity	lbs/hr
Y	expansion factor	dimensionless
β	ratio of orifice diameter to inside pipe diameter	dimensionless
$(1-\epsilon)$	particle fraction	dimensionless
θ	time	hr
$\overline{\theta}$	average contact time	hr
μ	dynamic viscosity of fluidizing medium	lb/ft-hr

Symbol	Definition	Dimension
ρ_g	density of the fluidizing medium	lbs/ft^3
ρ_s	density of solid material	lbs/ft^3
ρ_1	density of upstream air	lbs/ft^3

BIBLIOGRAPHY

1. Perry,R.H., Chemical Engineers' Handbook, 5th Edition, McGraw-Hill Book Co., New York, 1973.

2. Horio,M. and C.Y. Wen, A.I.Ch.E. Symposium Series, v73:n16(1977).

3. Kunii, D. and O. Levenspiel, Fluidization Engineering, John Wiley and Sons, Inc., New York, 1969.

4. Levenspiel, O., Chemical Reaction Engineering, John Wiley and Sons, Inc., New York, 1962.

5. Leva, M., Fluidization, McGraw-Hill Book Co., New York, 1959.

6. El-Kaissy, M. and G. M. Homsey, A.I.Ch.E Symposium Series, v73:n161(1977).

7. Levenspiel, O. and J. S. Walton, Chem. Engr. Progr. Symp., v50:n9,1(1954).

8. Mickley, H. S. and D. F. Fairbanks, A.I.Ch.E Journel, 1,374(1955).

9. Ziegler, E. N., L. B. Koppel, and W. T. Brazelton, Ind. Eng. Chem. Fundamentals, 3,324(1964).

10. Genetti, W. E. and J. G. Knudsen, I. Chem. Eng. Symp. Series, 30, 147(1968).

11. Vreedenberg, H. A., Chem. Eng. Sci., 9, 52(1958).

12. Bartel, W. J., W. E. Genetti, and E. S. Grimmett, A.I.Ch.E. Symposium Series, v:67,n:116(1971).

13. Chen, J. C. and J. G. Withers, "An Experimental Study of Heat Transfer from Plain and Finned Tubes in Fluidized Beds", A.I.Ch.E paper no. 34, 15th National Heat Transfer Conference, San Francisco (1975).

14. Chen, J. C., "Heat Transfer to Tubes in Fluidized Beds", A.S.M.E. paper no. 76-HT-75, 16th National Heat Transfer Conference, St. Louis(1976).

15. Bartel, W. J. and W. E. Genetti, A.I.Ch.E. Symposium Series, v69:n128(1973).

16. Priebe, S. J. and W. E. Genetti, A.I.Ch.E. Symposium Series, v73:n161(1977).

17. Kratovil, M. T., M.S. Thesis, Montana State University (1976).

18. McCabe, W. L. and J. C. Smith, Unit Operations of Chemical Engineering, McGraw-Hill Book Co., New York, 1976.

19. Kreith, F., Principles of Heat Transfer, Intext Press, Inc., New York, 1973.

20. Keairns, D. L., Westinghouse Research Laboratories, Pittsburg, Pennsylvania.

MONTANA STATE UNIVERSITY LIBRARIES
3 1762 10013632 2

N378
Ev26
cop.2

Everly, David W
Heat transfer from spiral tubes in an air fluidized bed

DATE	ISSUED TO

N378
Ev 26
cop. 2